

Equilibrium, kinetics, and thermodynamic studies on the biosorption of Reactive Red 120 dye utilizing the biomass of *Enterobacter sp.* MMO5

Salihu Yahuza^{a,b*}, Motharasan Manogaran^{a,d}, Nur Adeela Yasid^a, Ahmad Razi Othman^c,
Mohd Yunus Abd Shukor^a

^aFaculty of Biotechnology and Biomolecular Science, Department of Biochemistry, Universiti Putra Malaysia, 43400
UPM Serdang, Selangor, D. E, Malaysia.

^bDepartment of Microbiology and Biotechnology, Faculty of Science, Federal University Dutse, P. M. B. 7156, Dutse, Jigawa State, Nigeria.

^cDepartment of Chemical Engineering, Faculty of Engineering and Built Environment, Universiti Kebangsaan Malaysia, 43600
UKM Bangi, Selangor, D.E, Malaysia.

^dMalaysia Genome and Vaccine Institute, National Institute of Biotechnology Malaysia (NIBM), Jalan Bangi, 43000
Kajang, Selangor, Malaysia

Received 11th October 2024 / Accepted 24th December 2024 / Published 31st December 2024

Abstract. Biosorption using sustainable biomass such as bacteria is highly desirable due to their large surface area. *Enterobacter sp.* MMO5 was the organism of choice for the Reactive red-120 dye biosorption. The dye sorption optimization was done using Response Surface Methodology (RSM) and One-Factor-At-Time (OFAT). Upon RSM optimization, 50 mg/L, 150 rpm, 60 min, 7.0, and 45°C were the optimum results for the concentration, agitation, time, pH, and temperature, respectively. The biosorbent was characterized using Fourier Transform Infrared (FTIR) and Scanning Electron Microscopy (SEM) analyses. Biosorption isotherms, kinetics, and thermodynamic parameters were studied using nonlinear regression. Compared to the traditional One-factor-at-a-time (OFAT) method, the adsorption rate was about 6% higher after optimization using response surface methodology via Central Composite Design (CCD). The pseudo-second-order kinetics reaction fitted the dye biosorption with the lowest *AICc* and highest *adjR*² values. Langmuir, Freundlich, Henry, BET, Sips, Toth, Fritz-Schlunder IV, and Fritz-Schlunder V were the mathematical isotherm models with the best fit. Except for Henry, all the isotherm models tested on the RR-120 dye provided significant fitting results. Freundlich isotherm was the best after statistical analysis, having the lowest *AICc* value of -51.54. The thermodynamic parameters were computed using non-linear regression based on the vant Hoff plot. The enthalpy change (ΔH°) value was 52.91 kJ/mol, indicating that the reaction was endothermic. The adsorption process was spontaneous and thermodynamically feasible, as denoted by the negative values of Gibbs free energy (ΔG°) calculated at various temperatures. An increase in the degree of randomness at the solid/liquid interface was indicated by the positive entropy change (ΔS°), which is likely due to the structural changes in the bacterial biomass and Reactive Red 120 dye upon binding. This study demonstrated the potential of the bacterial biomass as a good biosorbent for dye biosorption, particularly Reactive Red 120, and offers a promising alternative for the bioremediation of textile dyes.

Keywords: biosorption, Reactive Red 120, *Enterobacter sp.*, kinetics, thermodynamic, optimization

INTRODUCTION

Eliminating contaminants from a solution using biological material is known as biosorption. These pollutants can be organic, gaseous, soluble,

inorganic, or insoluble. It is a physicochemical process comprising adsorption, absorption, surface complexation, ion exchange, and precipitation, especially metal ions, where reduction often leads to insolubility. Both living

*Author for correspondence: Salihu Yahuza, Department of Microbiology and Biotechnology, Federal University Dutse, PMB 7156, Dutse, Jigawa, Nigeria.

Email – salihu.yahuza@fud.edu.ng

and dead biomass have this attribute (Gadd, 2009). Because of its effectiveness and potential for recovery, biosorption is considered to be an efficient and fast method for removing and detecting pollutants from water, as opposed to biodegradation. Large amounts of wastewater, typically containing synthetic colors, are released by industries that manufacture paper, textile, printing, and paint products. In addition to being poisonous, teratogenic, and carcinogenic, the majority of these colors also have adverse consequences that include skin allergic dermatitis and cellular abnormalities. They also color wastewater streams, which block sunlight and eventually reduce aquatic plants' ability to participate in photosynthesis (Naskar and Majumder, 2017). The textile and pigment industries produce dyes that make wastewater challenging to treat due to their high levels of TSS (total dissolved solids), alkaline properties, high levels of biological oxygen demand (BOD), and Chemical Oxygen Demand (COD). The release of harmful dye effluents results an increase in the legislation and regulations of dye usage imposed by regulatory agencies to mitigate its harmful outcomes on the environment (Srinivasan and Viraraghavan, 2010).

Humans and marine life across the globe are seriously threatened by aquatic pollution, which is caused by dye contamination. These substances or the broken-down metabolites they produce have the potential to be poisonous, carcinogenic, and mutagenic. In addition to their toxic, carcinogenic, and non-biodegradable characteristics, dyes are highly undesirable even at low concentrations (< 50 ppm) in water bodies because they negatively impact the water ecosystem and interfere with aquatic organisms' ability to photosynthesize (Baldikova *et al.*, 2019).

Reactive dyes have the ability to react directly with fabric, resulting in a chemical interaction between the fabric molecules and the dyes that effectively dye the cloth. Synthetic dyes known as reactive Red 120 and Reactive blu-bezaktiv-150 have been used for a very long period in a variety of industries, most notably in the dyeing of clothing and shoes. The use of reactive dyes in dyeing processes produces a vast quantity of unfixed dyes, and the effluent produced as an additional result using this procedure may have an adverse effect on the ecosystem through effluent

discharges. According to the survey, almost 20% of the world's output is wasted during dyeing and dumped in the wastewater (Navaei *et al.*, 2019). Despite substantial advances in understanding complicated phenomena and a large number of publications in this field, marketing biosorption technologies remain a developing worldwide market (Fomina and Gadd, 2014). Commercialized biosorbents such as AlgasorbTM, AMT-BIOCLAIMTM (MRA), and Bio-fix were sold in the early 1990s. The biosorption technique is essential because of its ability to adhere to pollutants on various biological materials. The biosorption mechanism differs because different sorbents have different biological resources. The B.V. SORBEX commercialized biosorbent utilizes organisms such as *Ascophyllum nodosum*, *Sphaerotilus natans*, *Halimeda opuntia*, *Chondrus crispus*, *Palmyra pamata*, and *Chlorella vulgaris* in form of powder or granules that have affinity to toxic heavy metals where systems that are entirely mixed, fluid bed systems and fixed bed systems are utilized. On the other hand, AMT-BIOCLAIMTM utilizes *Bacillus* sp., which can be used to extract metals such as gold, cadmium, and zinc from waste cyanide solutions. The system consists of extruded polyethyleneimine beads that has been treated with glutaraldehyde and caustic soda. Its application is either in the fixed-bed canisters or fluid-bed reactor system. Furthermore, BIO-FIX^R uses bacteria, sphagnum peat moss, yeast, algae, and aquatic flora in the form of immobilized polysulfone. This product is claimed to be selective for heavy metals (Fomina and Gadd, 2014). Biological approaches to treating wastewater contaminated with dye have not yet been completely developed. As a technique for treating aqueous wastewater, adsorption is becoming increasingly common. Activated carbon forms the most frequently utilized sorbent and is considered as powerful adsorbent. Its high costs, especially in developed countries, prevented its application, which necessitated researchers to look for alternative techniques, particularly the employment of bacteria that are capable of using food and agricultural residual wastes as a growth substrate, which enables the sustainable production of the bacterial biosorbents (Karthik *et al.*, 2016). This study is justified as it addresses the high cost and limited accessibility of activated carbon for dye

removal by utilizing *Enterobacter* sp. MM05 biomass as a low-cost, sustainable alternative. It complements existing technologies, focusing on reactive dye biosorption, offering an eco-friendly solution for bioremediation wastewater treatment in textile industries.

MATERIALS AND METHODS

Reagents, chemicals and equipment

Sigma Aldrich Co., USA, produced the Reactive Red 120 (RR-120) dye that was chosen for this investigation. Additional materials utilized were of analytical grade and came from reliable vendors, including Fisher Scientific (Malaysia) and Merck (Germany). The dyes stock solutions were prepared at 1000 mg/L in deionized water. Each dye concentration was reconstituted with deionized water from a 1000 mg/L stock solution.

Harvesting bacterial biomass

Each of the twelve (12) isolates' biomass was collected and tested regarding the ability to absorb Reactive Red 120 dye. The isolates' day-old culture, which had an absorbance of approximately one at OD600, was centrifuged for 10 min at 10,000 ×g (Nwachukwu *et al.*, 2021). Before discarding the supernatant, each isolate's pellets were washed twice with Tris-buffer at pH 7.0. The cells in the pellets were rendered dormant by incubation at 60°C for 1 hour (Cheng *et al.*, 2020). They were later used in the investigation of Reactive Red 120 dye biosorption.

Bacterial biomass screening

To screen the bacterial biomass for dye sorption, 10 mL of Reactive Red 120 dye was combined with dried cells from the 12 bacterial biomass samples that had been inactivated in 50 mL flasks. The flasks were appropriately labeled and incubated at room temperature (25°C) with an agitation speed of 150 rpm. The monitoring of the adsorption potential of each bacterial biomass was carried out by taking out two (2) mL aliquots were obtained at regular intervals of 5 min for each flask, centrifuged for 10 min at 10,000 ×g, and the supernatant measured at A535 nm in a spectrophotometer (Li *et al.*, 2013; Chen *et al.*, 2020). Experiments were conducted in triplicate.

The percentage of the dye adsorption was determined using the formula below:

$$\text{Dye adsorption percentage (\%)} = \frac{A-B}{A} \times 100 \quad (1)$$

Where:

A= Absorbance prior to incubation

B= Absorbance after incubation

Optimization of Reactive Red 120 dye adsorption using one factor at a time (OFAT)

The highest adsorption percentage for Reactive Red 120 dye was observed in isolate 2, according to the screening results. Motharasan *et al.* (2021) previously identified and characterized this isolate as *Enterobacter* sp. strain MM05. To optimize the conditions for Reactive Red-120 dye adsorption utilising the isolate *Enterobacter* sp. strain MM05, one-factor-a-a-time (OFAT) approach was chosen. Using the OFAT method, the effects of contact duration, dye concentration, pH, adsorbent size, agitation speed, and temperature were all optimized. All of the parameters were tested one by one while keeping the earlier optimized parameters constant. Experiments were done in triplicate.

Optimization of Reactive Red-120 dye adsorption using response surface methodology (RSM)

In contrast to OFAT, the response surface approach optimizes and studies correlations between various bioprocess factors using a small number of tests (Das and Mishra, 2017; Gopalakrishnan *et al.*, 2020). It is a set of mathematical and statistical methods to determine the relationship between the answer and the independent variables. Several factors in bioremediation processes were successfully optimized using the RSM (Manogaran *et al.*, 2021; Lim *et al.*, 2014). The technique employed both the Plackett-Burman design (PBD) and the Central Composite Design (CCD). The PBD optimization was utilized to identify the important parameter(s) for Reactive Red 120 dye adsorption, which were then optimized using the CCD approach (Singh *et al.*, 2011). The Design-Expert 6.0.8 program investigated the experimental design and conducted statistical analysis (Das and Mishra, 2017).

Optimization using Plackett-Burman design and central composite design (CCD)

Six (6) distinct parameters were initially screened using PBD; the high and low values were initially obtained based on OFAT. They include dye concentration (40-100 mg/L), contact time (30-70 min), pH (6- 8.5), agitation speed (100-150 rpm), temperature (30-45 °C), and adsorbent amount (0.5 – 1.5 mL). The significant parameters were further optimized using CCD.

Validation of experiment

The Design-Expert software's anticipated adsorption response was validated using the CCD. The most significant parameter values were utilized to validate the experimental results. As a result, the actual percentage adsorption of Reactive Red 120 dye by *Enterobacter* sp. MMO5 was determined and compared to the expected value (Lim *et al.*, 2013).

Adsorption kinetics models

Based on the results of OFAT and RSM under ideal conditions, a batch kinetics experiment for Reactive Red 120 dye adsorption was performed at various dye concentrations. The concentrations were from 10 to 150 mg/L. The supernatant was analyzed at various time intervals using a spectrophotometer set to a particular wavelength (535 nm). Absorbances were recorded and plotted by a graph. Some previously verified adsorption kinetics models were employed for the Reactive Red 120 dye adsorption kinetics modeling (Çelekli *et al.*, 2019). The amount of adsorption q_t (mg/g), at a time t was determined utilizing the formula below:

$$q_t = \frac{(C_0 - C_t)}{W} V \quad (2)$$

The pseudo-first-order kinetic (Ho, 2004), the Elovich kinetic model (Cope, 1972), and the pseudo-second-order kinetic model (Ho, 2006) were the kinetic models utilized in this study. In order to predict the adsorption kinetics in the liquid phase, non-linear regression models are better suited than the linear model.

Biosorption isotherm models

The isotherm models (Table 1) describe the relationship in relation to the ratio of dye adsorbed to dye concentration remaining in a solution at a constant temperature under certain conditions. After a batch adsorption experiment at a series of concentrations of dye from 10 to 150 mg/L, the optimum isotherm for the Reactive red-120 dye adsorption can be determined (Iran *et al.*, 2017; Velkova *et al.*, 2018; Sarim *et al.*, 2019).

The equation below describes the Langmuir isotherm model:

$$q_e = \frac{q_{mL} b_L C_e}{1 + b_L C_e} \quad (3)$$

Where:

q_e = adsorbent dye equilibrium (mg/g)

q_{mL} = monolayer adsorbent capacity (mg/g)

C_e = dye equilibrium of the sorbate (mg/L)

b_L = Langmuir constant

The Freundlich isotherm, on the other hand, describes the surface of the sorbent as a non-uniform system with varying sites of different affinities (Dan-Iya, Adamu, *et al.*, 2023). Its equation is as follows:

$$q_e = K_F C_e^{\frac{1}{n_F}} \quad (4)$$

Where:

q_e = adsorbent dye at equilibrium (mg/g)

C_e = dye equilibrium of the sorbate (mg/L)

K_F =Freundlich constant

Brunauer-Emmett-Teller (BET) isotherm describes multilayer adsorption at the adsorbent surface (Asgher, 2012). It could be deduced from the Langmuir equation for each layer that the layer does not have to be completed before proceeding to the next one. The equation is as follows:

$$q_e = \frac{q_{mBET} \alpha_{BET} C_e}{(1 - \beta_{BET} C_e)(1 - \beta_{BET} C_e + \alpha_{BET} C_e)} \quad (5)$$

Table 1. Adsorption isotherm models with their formulae.

Model	Parameter	Formula	Reference
Henry	1	$q_e = HC_e$	(Ridha and Webley, 2009)
Langmuir isotherm	2	$q_e = \frac{q_{mL}b_L C_e}{1 + b_L C_e}$	(Langmuir, 1918)
Freundlich isotherm	2	$q_e = K_F C_e^{\frac{1}{n_F}}$	(Schirmer, 1999)
Dubinin-Radushkevich isotherm	2	Incorrect form $q_e = q_{mDR} \exp \left\{ -K_{DR} \left[RT \ln \left(1 + \frac{1}{C_e} \right) \right]^2 \right\}$ correct form $q_e = q_{mDR} \exp \left\{ -K_{DR} \left[RT \ln \left(\frac{C_s}{C_e} \right) \right]^2 \right\}$	(Radushkevich, 1949; Dubinin, 1965) (Mahanty <i>et al.</i> , 2023; Mudhoo and Pittman, 2023)
Smith isotherm	2	$q_e = W_{s1} - W_{s2} \ln(1 - C_e)$	(Dan-Iya, Adamu, <i>et al.</i> , 2023)
Redlich-Peterson isotherm	3	$q_e = \frac{K_{RP1} C_e}{1 + K_{RP2} C_e^{\beta_{RP}}}$	(Redlich and Peterson, 1958)
BET isotherm	3	$q_e = \frac{q_{mBET} \alpha_{BET} C_e}{(1 - \beta_{BET} C_e)(1 - \beta_{BET} C_e + \alpha_{BET} C_e)}$	(Liu, 2008)
Vieth-Sladek isotherm	3	$q_e = \frac{q_{mVS} b_{VS} C_e}{(1 + b_{VS} C_e)^{n_{VS}}}$	(Vieth and Sladek, 1965)
Unilin isotherm	3	$q_e = \frac{q_{mU}}{2b_U} \ln \left(\frac{a_U + C_e e^{b_U}}{a_U + C_e e^{-b_U}} \right)$	(Adamu <i>et al.</i> , 2023)
Khan isotherm	3	$q_e = \frac{q_{mK} b_K C_e}{(1 + b_K C_e)^{a_K}}$	(Dan-Iya, Adamu, <i>et al.</i> , 2023)
Toth isotherm	3	$q_e = \frac{q_{mT} C_e}{(K_T + C_e^{n_T})^{n_T}}$	(Adamu <i>et al.</i> , 2023)
Fritz-Schlunder-III isotherm	3	$q_e = \frac{q_{mFS} K_{FS} C_e}{1 + q_{mFS} C_e^{n_{FS}}}$	(Fritz and Schluender, 1974)
Radke-Prausnitz isotherm	3	$q_e = \frac{q_{mRP} K_{RP} C_e}{(1 + q_{mRP} C_e)^{n_{RP}}}$	(Dan-Iya, Adamu, <i>et al.</i> , 2023)
Brouers-Sotolongo	3	$q_e = q_{mBS} (-K_{BS} C_3^{n_{BS}})$	(Dan-Iya, Khayat, <i>et al.</i> , 2023)
Vieth-Sladek isotherm	3	$q_e = \frac{q_{mVS} b_{VS} C_e}{(1 + b_{VS} C_e)^{n_{VS}}}$	(Adamu <i>et al.</i> , 2023)
Parker isotherm	4	$q_e = q_{mP} \left[-a_P \left(RT \ln \frac{C_s}{C_e} \right)^{b_P} \right]$	(Parker, 1995)
Fritz-Schlunder-IV isotherm	4	$q_e = \frac{A_{FS} C_e^{\alpha_{FS}}}{1 + B_{FS} C_e^{b_{FS}}}$	(Fritz and Schluender, 1974)
Weber-van Vliet isotherm	4	$C_e = P_1 q_e^{(P_2 q_e^{P_3} + P_4)}$	(Dan-Iya, Khayat, <i>et al.</i> , 2023)
Marczewski-Jaroniec isotherm	4	$q_e = q_{mMJ} \left(\frac{(K_{MJ} C_e)^{n_{MJ}}}{1 + (K_{MJ} C_e)^{n_{MJ}}} \right)^{\frac{m_{MJ}}{n_{MJ}}}$	(Dan-Iya, Adamu, <i>et al.</i> , 2023) (Dan-Iya, Adamu, <i>et al.</i> , 2023)
Fritz-Schlunder-V isotherm	5	$q_e = \frac{q_{mFS5} K_1 C_e^{\alpha_{FS}}}{1 + K_2 C_e^{\beta_{FS}}}$	(Dan-Iya, Khayat, <i>et al.</i> , 2023)

Biosorption thermodynamic studies

Batch adsorption studies at various temperatures (30 to 50 °C) were employed to investigate how temperature impacted the Reactive Red 120 dye adsorption rate. Dye concentrations from 10 to 100 mg/L were used in thermodynamic batch adsorption studies (Tan and Hameed, 2017; Monte Blanco *et al.*, 2017; Yahuza *et al.*, 2020). The thermodynamic parameters were the Gibbs free energy (ΔG°), enthalpy (ΔH°), and entropy (ΔS°). Their equations are as follows:

$$\Delta G^\circ = -RT \ln KL \quad (6)$$

$$\Delta G^\circ = \Delta H^\circ - T\Delta S^\circ \quad (7)$$

$$K_C \approx \frac{K_L \left(\frac{L}{mol}\right) \times C^\circ \left(\frac{mol}{L}\right)}{\gamma} \quad (8)$$

$$\ln K_C = \frac{-\Delta H^\circ}{R} \times \frac{1}{T} + \frac{\Delta S^\circ}{R} \quad (9)$$

Where $R = 0.00831 \text{ kJ/mol} \times \text{K}$

To determine the thermodynamic parameters of adsorption (ΔG° , ΔH° , and ΔS°) the van't Hoff equations were utilized in this study. When adsorption achieves equilibrium, it is anticipated that the free energy change (ΔG) is equal to zero. When this occurs, Equation (6) converts to Equation (7), which is generally employed to calculate the ΔG° (standard Gibbs energy change).

Kinetic analysis was utilized first to obtain the Langmuir equation (8), followed by thermodynamic evaluation. The study of the two phases equilibrium constant, K_C , is directly contingent on the precise calculation of thermodynamic parameters (Tran *et al.*, 2016).

$$q_e = \frac{q_{mL} K_L C_e}{1 + K_L C_e} \quad (10)$$

RESULTS AND DISCUSSION**Dyes and bacterial biomass screening**

The Juru river banks in Pulau Penang, Malaysia, were the source of the bacterial isolates (Manogaran *et al.*, 2021). Figure 1 explains the

screening results versus the Reactive Red 120 dye. The Reactive Red 120 dye adsorption percentages vary between isolates as follows: Isolate 34XR (62.50%), Isolate 34XW (57.14%), Isolate 52 (37.5%), Isolate 2 (67.86%), Isolate 7 (41.07%), Isolate 29 (19.64%), Isolate 8 (12.5%), Isolate 30 (1.79%), Isolate 4 (28.57%), Isolate 1 (35.71%), Isolate 5.2 (50.00%), and isolate 5.1 (60.71%). Isolate 2 showed the highest adsorption percentage of 67.86% of the twelve isolates. All isolates, however, revealed the ability to adsorb the Reactive Red 120 dye from the solution. It has been observed that the majority of these isolates undergo decolorization or growth on Reactive Red 120 dye (Manogaran *et al.*, 2021). In addition, it has been shown that bacterial biomass has the ability to adsorb various groups of dyes in previous studies (Table 2). Wang *et al.* (2009) reported the use of *Enterobacter* sp. in the decolorization of reactive black 5 dye, having 92.56% decolorization efficiency with a maximum decolorization. However, Manogaran *et al.*, (2021) recently isolated and characterized the bacterial isolate (Isolate 2). The isolate was identified to be rod-shaped, Gram-negative, methyl red-negative, oxidase-negative, indole-negative, indole-negative, oxidase-negative, methyl red-negative, and Voges-Proskauer-positive that lives in water, sewage, soil, plants, and human and animal feces. It was further characterized using the 16S-ribosomal RNA sequencing technique with a gene sequence of 1,439bp linear DNA and accession number MW031860.1 GI: 1908125037 (Manogaran *et al.*, 2021). Bacteria can be utilized as a cheap biosorbent for pollutant removal. The ability of dead or inactivated cells of filamentous bacterium *Aureispira* sp., has been reported in the adsorption of the congo red dye and metal ions (Aragaw and Bogale, 2021).

A one-factor-at-a-time (OFAT) approach to optimizing the adsorption of Reactive Red 120 dye

The one-factor-at-a-time (OFAT) approach has long been the essential technique that has been widely applied in scientific and technical research. It works by adjusting one-factor level at a time and keeping the last values constant (Aragaw and Bogale, 2021). The technique was employed to investigate various environmental factors that

affect the biosorption of Reactive Red 120 dye. The optimum adsorption capacity of 42.14% was obtained at 50 mg/L.

Effect of initial Reactive Red 120 dye concentration

The adsorption sites decrease as the concentration increases, and the dye removal becomes more contingent on the initial dye concentrations

(Santos and Boaventura, 2008). A batch experiment was conducted using Reactive Red 120 dye at various concentrations ranging from 5 to 150 mg/L (Figure 2). Also, as the concentration was increased, the adsorption percentage decreased. This happens because the biosorbent's binding sites are entirely saturated on its surface (Horciu *et al.*, 2020).

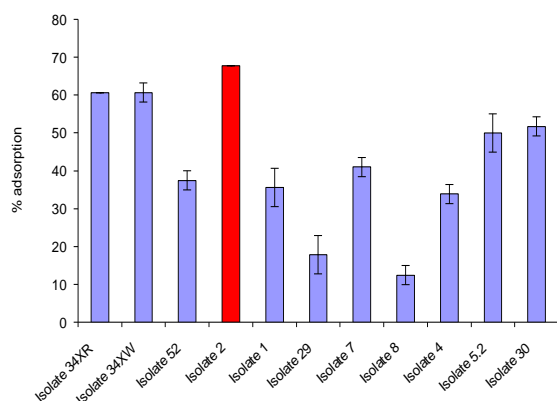


Figure 1. Screening results of Reactive Red 120 dye by twelve (12) bacterial isolates.

Table 2. Reactive Red 120 dye adsorption by various adsorbents.

Type of adsorbent	Best kinetics model	Best isotherm model	Qm values (mg/g)	RSM utilized	Sample matrices Tested	References
Pumpkin husk	Logistic	Langmuir	98.61	No	No	(Çelekli <i>et al.</i> , 2014)
Mesoporous magnetic carbon composite	Pseudo-second-order	Langmuir	172.4	Yes	No	(Jafari <i>et al.</i> , 2016)
<i>Spirogyra majuscula</i>	Pseudo-second-order	Freundlich	351.97	No	No	(Çelekli <i>et al.</i> , 2009)
Alumina-silica nanofibrous membrane	Intraparticle diffusion	Langmuir	884.95	No	No	(Bin Mukhlish <i>et al.</i> , 2017)
<i>Jatropha carcus</i> shells	General order	Liu	65.63	No	Yes (simulated dyehouse effluent)	(Prola <i>et al.</i> , 2013)
<i>Ulva prolifera</i> -derived biochar	Pseudo-second-order	Langmuir	107.13	No	No	(Mahendran <i>et al.</i> , 2023)
Crosslinked polystyrene resin	Not specified	Not specified	0.34-0.41g/g	No	No	(Bildik <i>et al.</i> , 2014)
Lentinus sajor-caju biomass	Pseudo-second-order	Feundlich, Temkin	182.9	No	No	(Arica and Bayramoğlu, 2007)
Chitosan formyl-sucrose sorbents	Not specified	Not specified	7g/g	No	No	(Mu <i>et al.</i> , 2023)
Hydrilla verticillata biomass	Pseudo-second-order	Freundlich	105mg/L	No	No	(Vij <i>et al.</i> , 2021)

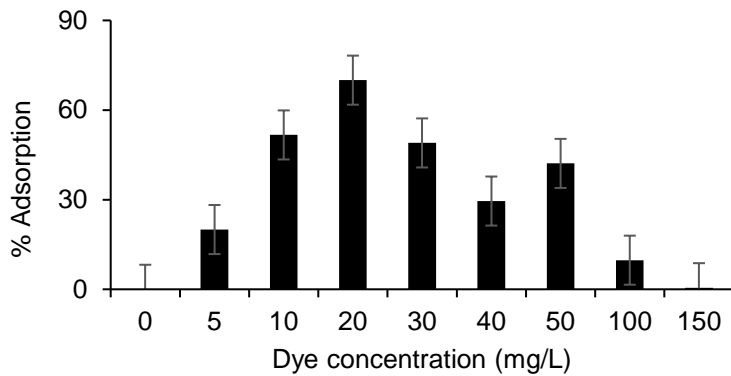


Figure 2. Dye concentration effect on the adsorption of Reactive Red 120 by the biomass of *Enterobacter sp. MM05*

pH effect

The pH affects the chemistry of the dye solution as well as the activity of functional groups in the biosorbent. It also affects the structural stability of the dye molecules (Cheruiyot *et al.*, 2019). Interactions involving the dye, a pollutant, and the adsorbent (biomass) are also affected by the structures of the dye and the bacterial biomass. Furthermore, basic (cationic) colors and acidic (anionic) dyes can be separated. These two groups make determining pH in dye adsorption research much more difficult. The adsorbent charge is initially amphoteric when the surface charge varies with the solution (Nouri *et al.*, 2021). The adsorption capacity is higher at 6.5 pH (47.77%) and lower at pH 7.5 (30.45%) (Figure 3). As the pH rises to 8.5, the % of dye removal declines drastically.

The surface of the biosorbent usually becomes positively charged as the pH decreases, which inhibits cationic species biosorption. However, as the solution's pH increases, the adsorbent's surface converts to a negatively-charged surface, resulting in the oppositely charged adsorbate electrostatically interacting with the sorbent (Horciu *et al.*, 2020). Adsorption of basic dyes raises with a raise in the pH of the solution, whereas in acidic dyes, it decreases. Reactive Red 120 dye is an acidic azo dye that exhibits this attribute. Several studies have shown that the optimum pH level for the majority of biosorbents tends to be slightly acidic to neutral (4-7) regardless of the microorganisms (Giese *et al.*, 2020; Ribas *et al.*, 2020).

Effect of temperature

Figure 4 profiles the temperature effects ranging from 25 to 55 °C on the adsorption of Reactive

Red 120 dye (Canizo *et al.*, 2019). The percentage of dye removal was optimum at 40 to 45°C (31-51%). Because higher temperatures allow a greater rate of diffusion, numerous investigations have demonstrated that dye adsorption rises with increasing temperature. As shown in Figure 4 below, as temperature increases, the adsorption percentage increases, and the optimum temperature is attained at 45°C. This increase is due to the chemical reaction that has taken place between the adsorbate (Reactive Red 120 dye) and adsorbent (*Enterobacter sp. MM05* biomass). Bayramoglu and Yilmaz (2018) have reported that the chemical potential and solubility of the adsorbate are predisposed by an increase in temperature since the movement of the substance interacts more efficiently with the adsorbent's functional groups, thus enhancing the adsorbent's protonation and deprotonation.

Similarly, (Sheshdeh *et al.*, 2014) reported that an increase in temperature affects the sorption of basic red dye using nickel oxide nanoparticles, in which the adsorption percentage is improved.

Effect of speed of agitation

The adsorption activity is greatly affected by the agitation speed. It affects how the bulk solution's solutes are distributed and how the outer boundary layer is formed. Typically, dye adsorption is affected by the degree of agitation, which increases as the stirring rate accelerates. The agitation reduces the boundary layer resistance, increasing system mobility (Zhu *et al.*, 2010).

Figure 5 shows the effect of agitation speed on the biosorption of Reactive Red 120 dye by the biomass of *Enterobacter sp. MM05* from 0-200 rpm. According to this finding, the adsorption capacity

is greater at 150 rpm and lower at 200 rpm (Figure 5). Therefore, the adsorption capacity increases from 0 to 150 rpm and decreases as the speed increases.

Shroff and Vaidya (2011) conducted similar research that indicated how the rate of sorbent/sorbate agitation (60 to 210 rpm) affects the adsorption of Ni (II). The adsorption capacity decreased as the agitation speed was raised, whereas the removal efficiency increased to 150 rpm (15.83 mg/g). Maximizing the interaction between dyes and biomass binding sites can be achieved by increasing agitation. As a result, the adsorbent particles' external mass transfer barrier becomes thinner, allowing the sorbate ions to be transported to the sorbent sites. In contrast, (Mahmoud *et al.*, 2017) reported the highest

removal efficiency (80.8%) at a speed of 250 rpm. This could be related to adsorbent particle dispersion.

Furthermore, in research conducted by (Long *et al.*, 2017), the agitation speed of 120 rpm was enough to guarantee the access of every surface combining site needed for *B. cereus* to adsorb S_r (II) ions to their maximum potential. The mass transfer resistance that forms around the adsorbent particles can be reduced with appropriate agitation, making it easier for the metal ions and binding sites to make contact. Decreased biosorption at a lower agitation speed was most likely due to inadequate contact with the biosorbent particles, which caused the particles to stick together.

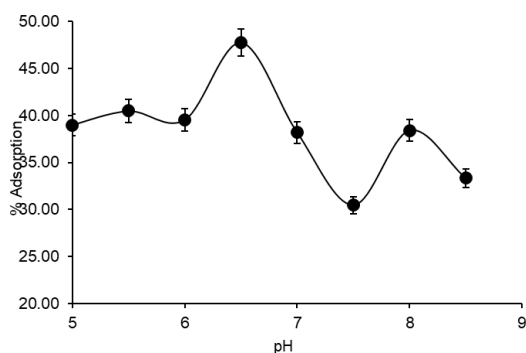


Figure 3. pH Effect on the Adsorption of Reactive Red 120 dye by the biomass of *Enterobacter sp.* MM05.

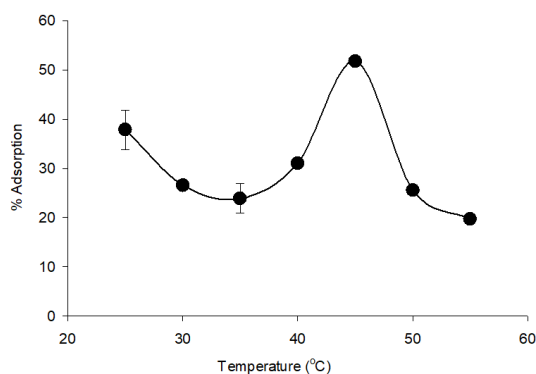


Figure 4. Temperature effect on the Adsorption of Reactive Red 120 by the biomass of *Enterobacter sp.* MM05.

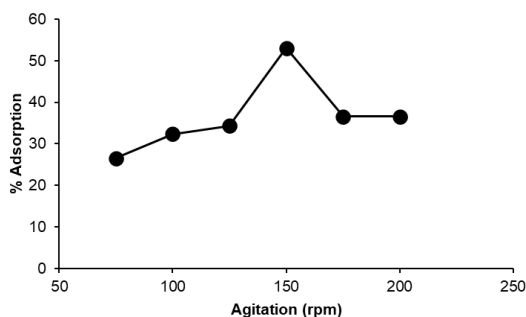


Figure 5. Agitation speed effect on the Adsorption of Reactive Red 120 by the biomass of *Enterobacter sp.* Strain MM05.

Effect of contact time

Time has a significant effect on the adsorption of dye (Figure 6). The dye adsorption was relatively fast in the first 30 min, then steadily plateaued as contact time was increased. After 60 min, there was no discernible variation in dye adsorbed. The equilibrium time was established at 60 min in batch adsorption experiments (Mohammadi *et al.*, 2011). Adsorption capacity generally increases with the increase in time until the dye solution's capacity is depleted, at which point it will reach equilibrium. The amount adsorbed indicates the maximal dye adsorption capacity of the bacterial biomass (Chatterjee *et al.*, 2010). An experiment was conducted at time intervals from 5 to 90 min) in order to assess how adsorption is affected by contact time. The results show that the maximum adsorption capacity occurred at 60 min (1 hour). The finding connects with the investigation conducted by Mohammadi *et al.* (2011), where the equilibrium time of methyl orange dye adsorption was found at 60 min.

Adsorbent dosage effect

Biosorbent dosage has a significant impression on the adsorption percentage. As the amount of biosorbent increased, so did the biomass's adsorption efficiency, increasing the adsorption percentage, as illustrated in Figure 7 (Rizzi *et al.*, 2014). The adsorbent amounts ranged from 0.5 to 1.5 mL. According to (Lim *et al.*, 2013), the greater the biomass surface area, the more adsorption sites. In a related study, Sulak and Yatmaz (2012) observed that the amount of adsorbent was increased from 0.25 to 3.0 grams, and it was found that the removal efficiency increased to 93%. Increased in the removal percentages was a result of adsorbent surface areas an active functional group increment. According to a study on the removal of cationic dyes using an alternative adsorbent, the dye removal increased with a concurrent decrease in particle size as the smaller the particles, the more surface area they possess (Santhi *et al.*, 2016).

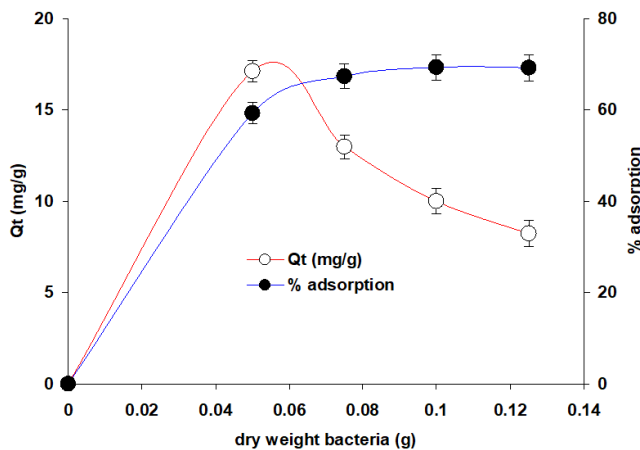


Figure 6. Effect of adsorbent dosage on the adsorption of Reactive Red 120 dye by the biomass of *Enterobacter sp.* MM05.

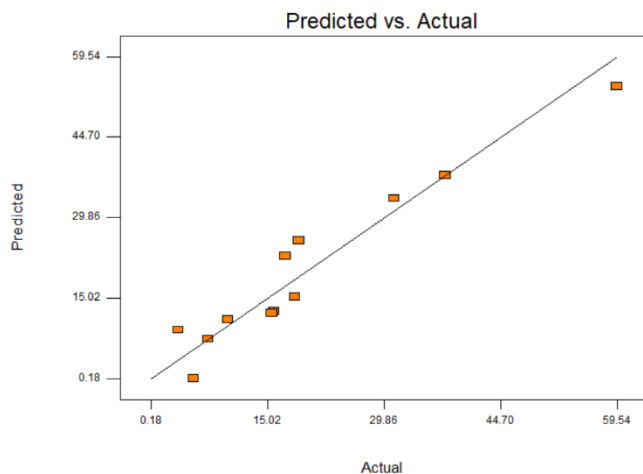


Figure 7. Similarity plot of actual and predicted adsorption values for Reactive Red 120 dye adsorption by *Enterobacter sp.*

To determine the influence of many parameters on dye removal, many researchers have employed an OFAT strategy (Liu *et al.*, 2014; Manogaran *et al.*, 2021). Mawad *et al.* (2021) have reported the optimum conditions of pH, contact time, temperature, adsorbent dosage, and initial dye concentration, of which environmental conditions played an important task in the adsorption process. A study has indicated that a contact time of 360 min was found to be the most favorable condition for the adsorption process (Nath *et al.*, 2015). In this study, OFAT-based optimization yields a temperature of 30°C, a biomass concentration of 0.5 g/L, and an initial dye concentration of 100 mg/L. As many researchers have reported the impact of environmental factors in enhancing the adsorption process, this finding is no exception.

Optimization of Reactive Red 120 dye adsorption using response surface methodology

The adsorption conditions of Reactive Red 120 dye under optimal conditions were further determined using the Plackett Burman Design and CCD.

Screening using Plackett Burman design (PBD)

One kind of preliminary or screening design is the Plackett-Burman design, of which R.L. Plackett and J.P. Burman developed the tool in 1946. Through the investigation of the influence that operational parameters have on the configurations of the system, the purpose of its creation was to simplify quality control in order to facilitate the making of intelligent decisions (Vanaja and Rani, 2007). In this study, the variables that significantly affect the adsorption of Reactive Red 120 dye were selected and established using the software Design Expert 6.0.8. The variables with a substantial impact on the dye adsorption process were chosen. They were temperature, adsorbent dosage, pH, contact time, agitation speed, and dye concentration. A total of 12 distinct tests were performed in the PBD utilizing the specified variables (Table 3). Those ranges that OFAT obtained served as the basis for the ranges used for each independent variable. Several researchers have used PBD as an alternative approach to experimental design and

optimization. Karlapudi *et al.* (2018), in their research finding, reported the use of PBD in their work, where the PBD was chosen to screen the important fermentation process components concerning their effects.

Furthermore, Ameenudeen *et al.* (2021) reported the employment of PBD in their research finding. (Manogaran *et al.*, 2018) uses PBD to optimize culture composition. Using the Design Expert software, both the experimental design and the statistical analysis of the data were carried out according to the established protocols (Design Expert software, version 6.0.8). The software indicated that run 6 had the lowest RR-120 dye biosorption (7.34%), while run 11 had the highest (57.36%). The PBD and dye percentage adsorption of Reactive Red 120 dye in 12 experimental runs are shown in Table 3.

In their research findings to optimize the adsorption of dye effluents, (Venkataraghavan *et al.*, 2020) utilized PBD and determined the significant factors accountable for the adsorption were pH, time, and dye concentration. The resultant experimental and predicted values were found to agree, and the coefficient of determination value (0.9818) implied that the model obtained was significant. They employed a Box-Behnken (BB) design for further optimization. In contrast, this finding showed that only two factors were significant (adsorbent amount and dye concentration). Therefore, a CCD was used to optimize the adsorption further. Figure 7 establishes the relationship plot between the predicted and actual adsorption values for the biosorption of Reactive Red 120 dye on the biomass of *Enterobacter* sp. MM05 in PBD.

Adsorption optimization for Reactive Red 120 dye using the CCD

A researcher can use this design to probe the effects of each factor and the resulting response, in addition to the results of interactions between factors on the response variable of each factor (Khammour *et al.*, 2016). This design further optimized the significant parameters identified in PBD (i.e., dye concentration and adsorbent amount). About 13 experiments were conducted for the two significant factors in PBD (dye concentration and adsorbent amount) at low and high levels. The highest adsorption capacity (72.65%) of the Reactive Red 120 dye was

recorded in run 3 (Table 4). The coefficient of determination estimates a model's accuracy (R^2). The R^2 is continuously in the interval of 0 to 1, and the value's magnitude can be used to denote the model's goodness of fit between the model experimental response variable and the predicted values. The R^2 value is always between 0 and 1

(Zhang *et al.*, 2017). It was determined that the R^2 value of the model was 0.9563, which was quite close to 1 (Table 5). This shows that the dye adsorption could explain 95.63% of the model's behavior. In addition to this, it is shown that the regression model was capable of explaining the majority of the data variation.

Table 3. PBD and dye percentage adsorption of Reactive Red 120 dye in 12 experimental runs.

Run	A. Dye conc. (mg/L)	B. Contact Time (mins.)	C. pH	D. Agitation (rpm)	E. Temperature (°C)	F. Adsorbent size (mL)	% Adsorption
1	100	20	8	100	45	1.5	24.80
2	100	20	4	150	25	0.5	9.22
3	40	5	4	100	25	0.5	20.93
4	40	20	8	150	25	1.5	46.67
5	100	5	8	150	25	1.5	26.59
6	100	20	4	150	45	0.5	7.34
7	100	5	8	100	25	0.5	10.98
8	40	5	4	150	45	1.5	47.67
9	40	5	8	150	45	0.5	21.25
10	100	5	4	100	45	1.5	28.04
11	40	20	4	100	25	1.5	57.36
12	40	20	8	100	45	0.5	25.00

Table 4. Experimental plan and result for the optimization of Reactive Red 120 dye adsorption using the three-level full factorial design.

Run	A: Dye concentration (mg/L)	B: Adsorbent amount (mL)	Actual value (%)	Predicted value (%)
1	100	1	20.28	26.66
2	70	1	41.92	39.65
3	40	1.5	72.65	73.49
4	70	1	43.43	40.65
5	70	0.5	3.54	4.12
6	70	1	38.13	37.65
7	70	1	43.43	41.47
8	70	1.5	52.27	51.99
9	100	1.5	41.57	41.01
10	100	0.5	8.63	9.01
11	40	1	55.56	57.15
12	70	1	43.43	44.67
13	40	0.5	39.74	38.63

Additionally, it was demonstrated that the model was relevant by the relatively high adjusted and predicted R^2 values of 0.9325 and 0.8763, respectively (Table 5), corresponding to an agreement between the actual and predicted values. Therefore, the model offered a wealth of information concerning the relationship between the independent variables and those dependent on some other factor. Similar results for the second-order RSM experiments based on Box Behnken and CCD have been reported by other researchers (Solomon *et al.*, 2020). A sufficient degree of precision was employed to test the signal-to-noise ratio, which was found to be 14.94, indicating that it was good (Table 5). The value emphasized the significance of the model to the process. (Manogaran *et al.*, 2018) have stated an adequate precision value of 31.14 in their studies on the optimization of media composition for the mineralization of glyphosate by *Burkholderia vietnamiensis* strain AQ5-12.

In order to ascertain the significance of using the model parameters, F and P values were used. As reported by Hassanzadeh-Tabrizi and Taheri-Nasaj (Manogaran *et al.*, 2018), in proportion to the magnitude of the F -value, the "prob > F " value will be smaller as the magnitude of the F -value increases., the more essential the corresponding coefficient. The models were found to be highly significant, according to the quadratic regression model (Table 5). A very low probability value of 0.001 was found to be

associated with the model's F -value for the adsorption of Reactive Red 120 dye, which was found to be 15.98 (Table 5). The model's F -value of this magnitude had a 0.001% chance of occurrence due to noise. Based on the $\text{prob} > F_i$ value, which was 0.0500, this suggested that the model terms were significant. Only A and B models were significant for the adsorption of Reactive Red 120 dye by the biomass of *Enterobacter* sp. MM05 in this case. The model's F -value declines abruptly, increasing the associated p -value to be slightly above the acceptable levels for significance. The lack of fit for the F and P values of the model were 0.26 and 0.16, respectively, indicating that it was not significant and that the models were adequate. Tables 4 and 5 show the plan of the experiment and optimization result for Reactive Red 120 dye adsorption, respectively, utilising a CCD design.

There is a high concurrency between the actual and predicted values from the CCD design (Figure 7). The predicted model value was highly correlated to the actual value. Equations 11 and 12 are the equations that illustrate them in terms of the actual and coded factors.

$$Y=47.00-1.36A+76.21B+0.006A^2-19.02B^2+0.004AB \quad (\text{Eqn. 11})$$

$$Y=37.65-16.24A+19.10B+5.26A^2-4.76B^2+0.006AB \quad (\text{Eqn. 12})$$

Table 5. RSM analysis of variance (ANOVA) for the CCD of the Reactive Red 120 dye adsorption

Source	Sum of Squares	df	Mean Square	F-value	Prob>F	
Model	3872.05	5	774.41	15.98	0.0010	significant
A	1583.30	1	1583.30	32.67	0.0007	
B	2187.91	1	2187.91	45.14	0.0003	
A ²	76.38	1	76.38	1.58	0.2497	
B ²	62.46	1	62.46	1.29	0.2936	
AB	0.00	1	0.00	0.00	0.9986	
Residual	339.28	7	48.47			
Lack of fit	233.68	3	77.89	0.26	0.1615	not significant
Pure Error	105.60	4	26.40			
Core Total	4211.34	12				
Std.	6.96		R-Squared	0.9563		
Mean	37.88		Adj R-Squared	0.9325		
C.V.	18.38		Pred R-Squared	0.8763		
PRESS	2047.23		Adeq Precision	14.94		

Adsorption of Reactive Red 120 dye in a three-dimensional (3D) response surface pattern

In order to shed light on the connections between the two independent factors and the dependent variable, three-dimensional (3D) response surface plots of the dependent variable can be utilized. These plots are valuable in describing the main effects of the two independent variables as well as the interaction effects (Manogaran *et al.*, 2018). The quadratic model was utilized in order to produce three-dimensional response surface plots for the responses. The purpose of these plots was to obtain an inherent understanding of the manner in which independent factors and their interactions impact the dependent variable. The 3D response surface plots show how the three process parameters affect the response parameter. Each plot shows how two important independent factors interact while keeping the other two constant. The plot contour depends on how the three independent components interact and affect percentage removal. The three-dimensional response surfaces and contour plots of the model for the interactions between the variables are displayed in Figure 8, where the significant independent variables (A) dye concentration and (B) sorbent amount towards the dependent variable (RR-120 dye removal percentage) from the experimental design. The utility of the CCD to optimize dye sorption to bacterial biomass is relatively absent from the literature, with many studies reporting the Box Behnken (BB) as a more frequent choice, perhaps due to BB having a reduced number of individual runs of the

experiment compared to CCD (Saha and Mazumdar, 2019). For instance, the Box-Behnken design has also been utilized in other dye adsorption studies employing bacterial biomass, such as optimizing Reactive Green-19 dye removal. The study investigated the effects of pH, temperature, and yeast extract concentration to determine optimal conditions for a bacterial consortium (Das and Mishra, 2017). In another study, the BB design successfully optimized the removal of Trypan Blue dye by the inactivated biomass of *Pseudomonas sp.* strain MM02 (Abubakar *et al.*, 2023).

RSM validation

The CCD result was utilised in the validation of the linear model. The optimal conditions for the dye adsorption were 48.8 mg/L and 1.38 mL dye concentration and adsorbent amount, respectively. RSM predicted a $76.88 \pm 1.13\%$ adsorption rate. To confirm the outcome predicted by the CCD, the optimal parameters that had been identified earlier were then used in an experiment that was carried out. Table 6 displays a comparison between the results that were predicted by RSM and those that were obtained through experimentation ($75.14 \pm 1.25\%$), where no statistical difference in the percentage of adsorption between the predicted and experimental value ($p > 0.05$) was observed. The maximum adsorption using OFAT was $69.78 \pm 1.03\%$, indicating that RSM resulted in an approximate 6% increase in adsorption.

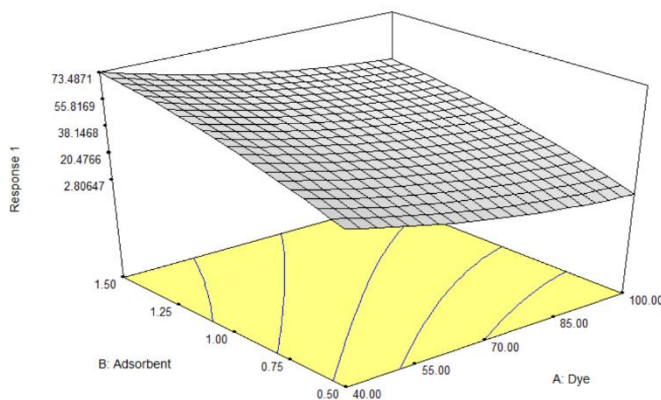


Figure 8. Three-dimensional (3D) response surface plots for Reactive Red 120 dye adsorption demonstrating the interactive effects of (A) Dye concentration and (B) Adsorbent amount.

Table 6. Comparison of RSM-predicted and experimental results for Reactive Red 120 dye and OFAT.

Factors	Name	Predicted levels	Experimental levels
A	Dye conc. (mg/L)	48.8	48.8
B	Adsorbent amount (mL)	1.38	1.38
		Predicted	Experimental
	Response (%) CCD	76.88±1.13	75.14±1.25
	Response (%) OFAT		69.78±1.03

Determination of adsorption kinetic models for Reactive Red 120 dye

An adsorption process's kinetics crucially describes the reaction's rate and mechanism. It is reliant on how the adsorbate and adsorbent interact. Given that the best biosorbent for use in adsorption studies must have a rapid and high adsorption capacity rate, the adsorption rate aids in this decision-making (Eris and Azizian, 2017). Additionally, it gives the adsorption process the time it needs to reach equilibrium. As a result, kinetic modeling is essential for research and system development for pollutant removal (Eris and Azizian, 2017). It is possible to express the controlling mechanism by using several different models, including mass transfer and chemical reaction (Eris and Azizian, 2017).

This study employed a batch kinetics experiment at various dye concentrations (10 to 150 mg/L) for about 90 min. The analysis of the kinetic studies was done using contact time-dependent of low and high dye concentrations based on the OFAT results. The pseudo-first-order and pseudo-second-order equations were used to analyze the adsorption data using non-linear kinetic regression. Regression via Non-linear regression was employed because it provides precise calculations (Basirun and Shukor, 2021). The kinetic models were documented as simple, robust, and capable of fitting experimental biotechnological data and supporting assumptions. Adsorption rate process is usually explained by either the pseudo-first-order (PFO) model or the pseudo-second-order (PSO) kinetic model (Basirun and Shukor, 2021). However, The PSO kinetic model could estimate the adsorption pattern better than the PFO model. This is because, in many adsorption systems studied, first-order kinetic models only apply to the very early stages of the adsorption process, and many results do not fit well across the entire adsorption

period (Moussout *et al.*, 2018). In addition, the PSO equation leads to the premature conclusion that chemisorption is the rate control step in the adsorption process (Moussout *et al.*, 2018).

The adsorption process of Reactive Red 120 dye by the biomass of *Enterobacter* sp. MM05 was then fitted to the PFO and PSO kinetic models (Figure 9). The finding indicated that adsorption models could be best fitted using the PSO kinetic model based on the result of error function analysis (Table 7). This is consistent with many published studies that report that PSO kinetics is the best model (Moussout *et al.*, 2018). (Gurav *et al.*, 2021) have reported pseudo-order kinetics as best model with R^2 value greater than 0.99. Similarly, (Taher *et al.*, 2018) reported the fitness of adsorption data to the pseudo-second-order kinetics in their finding. In contrast, some researchers have reported the use of a kinetic model to describe some scientific research that does not necessarily involve adsorption. For example, (Bilehal *et al.*, 2001) selected the PSO kinetic model to show the reaction dependence on the concentration of permanganate and ruthenium (III) in their research. Chemisorption is the process often prematurely associated with the second-order reaction's rate-controlling phase, which is connected to the chemical reaction (Tan and Hameed, 2017). In other words, the reaction's mechanism is chemically controlled. Adsorption kinetics are dominated by two competing reversible second order processes at higher adsorbate or adsorbent ratios (Bilehal *et al.*, 2001).

Determination of adsorption isotherm models for Reactive Red 120 dye

The isotherm investigation provides important physicochemical data for future assessment of the biosorption process in the laboratory under batch operation. As a result, isothermal studies and isothermal modelling are critical in maximizing

the effectiveness of the design for any adsorption parameter (Bilehal *et al.*, 2001). To select an acceptable model for the process design, accurate equilibrium data that fits appropriately into several isotherm models is required. The variable derived from various models provides critical information regarding the adsorption process’s mechanisms, adsorbent affinities, and surface properties that are not available from other sources information such as laboratory experiments. When designing an adsorption system for industrial use, it is critical to have this knowledge. To be most informative about intrinsic kinetics, which is chemical kinetics that occur on the adsorbent surface when there are no

transport constraints, the kinetic isotherm should be able to shed light on it (Tan and Hameed, 2017).

Before any progress can be made in understanding adsorption mechanism pathways and the practical systems design, adsorption isotherms must be thoroughly understood. When developing the best adsorption process plan, it is critical to determine the most proper correlation between the equilibrium curve and the data obtained from measurements (Monte *et al.*, 2018). The adsorption capacity must be precisely defined mathematically to generate accurate models about equilibrium adsorption variables and to construct comparisons of the biosorption behavior of various adsorbents (Hu *et al.*, 2021).

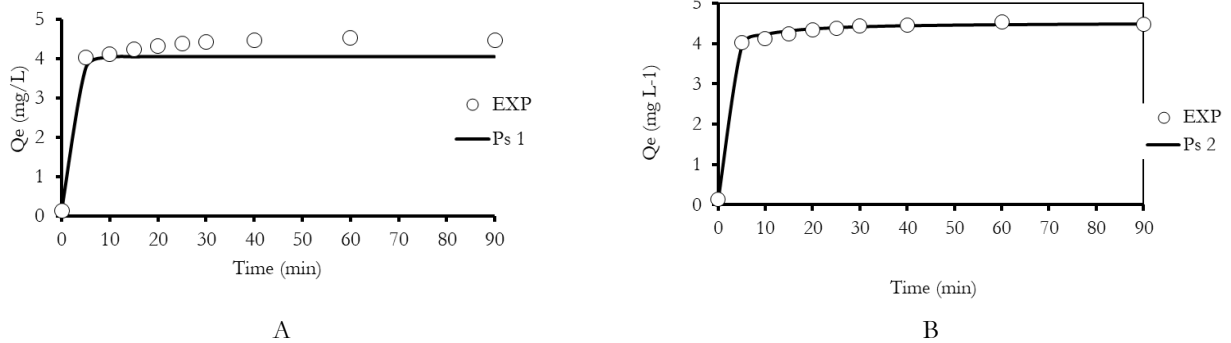


Figure 9. Adsorption profile of *Enterobacter sp.* strain MM05 biomass fitted to (A) Pseudo-first-order kinetic model and (B) Pseudo-second-order kinetic model for Reactive Red 120

Table 7. Statistical analyses of kinetic models for the adsorption of Reactive Red 120 dye.

Model	Parameter	RMSE	adR ²	AICc	BIC	HQC	AF	BF
Pseudo-first order	2	0.385	0.897	4.660	15.065	6.311	1.084	0.938
Pseudo-second order	2	0.057	0.998	39.091	49.497	50.743	1.025	1.014

Where:

RMSE =Root mean square error

p = Number of parameters

adR² =Adjusted coefficient of determination

BF = Bias factor

AF = Accuracy factor

AICc = Adjusted Akaike Information Criterion

BIC =Bayesian Information Criterion Information

HQC= Hannan–Quinn information criterion

Eight different isothermal models, including Henry, Freundlich, Langmuir, BET, Toth, Sips, Fritz Schlunder IV and Fritz Schlunder V were fitted to the equilibrium data from the batch adsorption studies. As shown in Figure 10, only Henry's isotherm model fails to fit the data. The Freundlich model was the best isotherm model based on the consensus statistical analysis, as shown in Table 8. Several researchers have reported Freundlich as the best isotherm model in the adsorption of dyes using different adsorbents.

For example, (Muthukumaran *et al.*, 2016) reported that the Freundlich isotherm model was able to fit the adsorption data with an R^2 value of 0.957. Also, (Felista *et al.*, 2020), in their adsorption work of Reactive Black 5 using macadamia seed husk (a plant adsorbent), the Freundlich isotherm was the best model. Furthermore, (Ali *et al.*, 2020) reported the fitting of adsorption data to the Freundlich isotherm model.

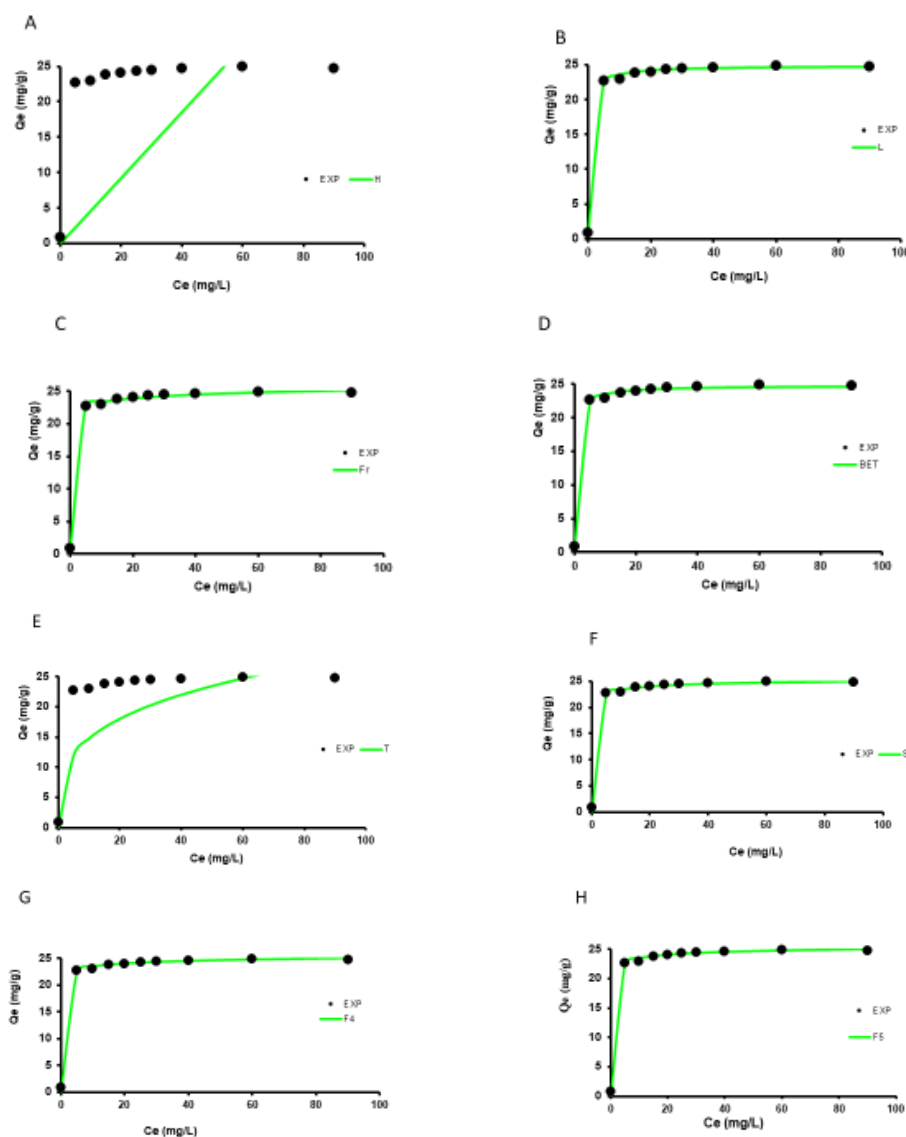


Figure 10. Equilibrium biosorption isotherm data of Reactive Red 120 dye by *Enterobacter sp.* MM05 modelled using (A) Henry, (B) Langmuir, (C) Freundlich, (D) BET, (E) Toth, (F) Sips, (G) Fritz Shlunder IV and (H) Fritz Schlunder V.

Table 8. Error function analysis for fitting the isotherm of Reactive Red 120 dye adsorption.

Model	p	RMSE	AdR ²	AICc	BIC	HQC	BF	AF
Henry	1	2.40	-0.41	24.15	18.74	18.10	0.35	3.27
Langmuir	2	0.05	1.00	-49.65	-59.05	-60.31	0.99	1.02
Freundlich	2	0.04	1.00	-51.54	-60.93	-62.20	0.98	1.02
BET	3	0.05	1.00	-41.71	-56.80	-58.70	1.00	1.01
Toth	3	1.15	0.06	21.17	6.08	4.17	0.53	1.94
Sips	3	0.06	1.00	-37.01	-52.10	-54.00	0.68	1.48
F4	4	0.07	1.00	-24.95	-48.74	-51.27	0.61	1.66
F5	5	0.08	1.00	-8.15	-46.63	-49.80	0.68	1.48

In contrast, many researchers have reported other isotherm models, such as Langmuir, Toth, and BET. For example, (Canizo *et al.*, 2019) reported the Langmuir isotherm model as the best model for fitting Crystal Violet adsorption data. Similarly, (Horciu *et al.*, 2020) have reported the fitting of reactive Brilliant Red HE-3B dye adsorption data to the Langmuir isotherm model. Other works have pointed to other models, such as the Toth model (Rusu *et al.*, 2022).

Studies of thermodynamics on the Reactive Red 120 dye adsorption

Establishing the adsorption processes is essential for adsorption research, including chemical or physical adsorption. Van der Waals forces and other relatively weak interactions cause physisorption, whereas stronger chemical bonds and consequent electron transfer from the adsorbent surface to adsorbate cause chemisorption to be dominant (Elsherif *et al.*, 2021). The thermodynamic characteristics of an adsorption activity determine its feasibility and spontaneity. The equilibrium K_c constant is essential for calculating these thermodynamic parameters. Gibbs free energy and other thermodynamic properties are calculated using the constant derived from partition constants, isotherm models, and distribution coefficients (Değermenci *et al.*, 2019).

The Langmuir constant, K_c , and nonlinear regression of the van't plot were used to determine the thermodynamic parameters according to (Nguyen *et al.*, 2020; Tran *et al.*, 2020) and (Chen *et al.*, 2021; Hu *et al.*, 2021) methods. Despite frequently using the linearized variant, the nonlinear van't Hoff plot was preferred. The main issue with models having linearized kinetics, isotherms, and thermodynamics is that they may

experience significant error deviations due to error distribution issues (de Oliveira Carvalho *et al.*, 2019). The 95% confidence interval in nonlinear regression is frequently smaller (de Oliveira Carvalho *et al.*, 2019). Five temperature data points (30, 35, 40, 45, and 50°C) were used in the thermodynamics research to maximize the effectiveness of nonlinear regression, which performs better when more data points are used. The kinetic and Langmuir equilibrium isotherms of Reactive Red 120 dye were processed at various temperature points for dye concentrations from 10 to 150 mg/L. According to the kinetics determination, a PSO model was chosen from statistical analysis. To compute the Langmuir constant, K_L , the isotherm model was plotted using the q_e constants from the PSO model. The Langmuir constant, K_L , is a dimensionless thermodynamic equilibrium constant that should be converted into a dimensionless form or K_C to be used in standard thermodynamic calculations (Moussout *et al.*, 2018; Tran, 2022). The region containing the actual information for adsorption equilibrium may be the Langmuir isotherm zone, which is distinguished by saturation at high concentrations. The Langmuir constant (K_L) is used instead of the thermodynamic equilibrium constant (K_C) to estimate the thermodynamic parameters. Table 9 shows the thermodynamics parameters of Reactive Red 120 dye adsorption.

The determining performance of the thermodynamic parameters throughout the adsorption process for Reactive Red 120 dye is summarized in Table 9. The entropy change (ΔS°) and enthalpy change (ΔH°) were obtained from the non-linear regression of the dimensionless K_c values versus temperature (Figure 11). As the temperature increased from 303.15 to 321.15 Kelvin, the Reactive Red 120 maximum

adsorption capacity value for the dye was decreased. This could either be due to a continuous increase in the broadening sorption site on bacterial biomass unfavorable to the dye molecule adsorbed or due to the mechanisms of desorption caused by poor adsorption contact throughout the adsorption phase (Silva *et al.*, 2020). In essence, as heat is transferred out of the system, an exothermic process results in $\Delta H < 0$, and as a result, the environment experiences a positive change in entropy. On the other hand, endothermic reactions have $\Delta H^\circ > 0$. As a result, as heat is introduced into the system, the

environment's entropy changes negatively (Abedi *et al.*, 2016). The Reactive Red 120 dye adsorption was endothermic with the positive ΔH° value (52.91 kJ/mol). The Gibb's free energy change (ΔG°) versus Temperature in Figure 12 with $-\Delta G^\circ$ values (Abedi *et al.*, 2016), demonstrates that the dye adsorption onto bacterial biomass biosorbent occurred spontaneously without or with little demand for energy and heat. Since chemisorption corresponds to adsorption with a $-\Delta G^\circ$ of -400 to -80 KJ/mol, the adsorption occurred through physisorption.

Table 9. Thermodynamics parameters of ΔG , ΔH , and ΔS determined from van't Hoff and Langmuir Dimensionless Plot for the Adsorption of Reactive Red 120 Dye.

Temp (K)	K_c	ΔG° (kJ/mol)	95% CI Lower	95% CI Upper	ΔH° (KJ/mol)	ΔS° (Kj/(mol.K))
303.15	4,6787	-38.4139	-40.18	-36.65	52.91	301.30
308.15	5,7180	-39.6608	-40.86	-38.46		
313.15	8,094,6	-41.2799	-42.05	-40.51		
318.15	10,919	-42.7485	-43.41	-42.09		
323.15	15,596	-44.4169	-44.83	-44.01		

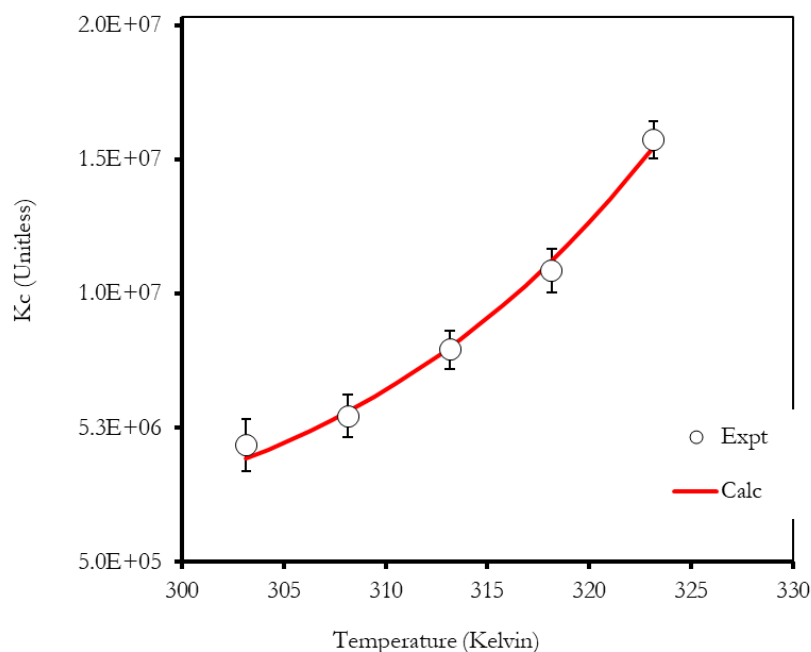


Figure 11. Non-linear van't Hoff plot of Dimensionless Constant, K_c against Temperature, K for RR-120 dye adsorption. Error bars are mean \pm standard error (n=3)

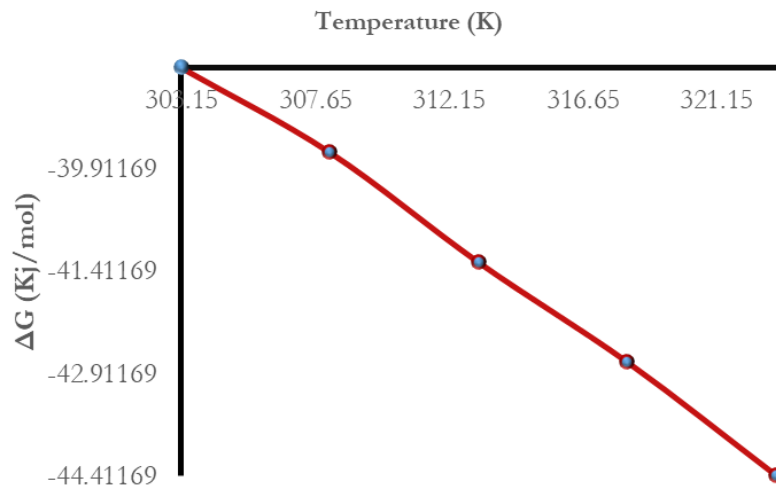


Figure 12. Gibb's free energy change (ΔG°) versus Temperature (K) Plot for RR-120 dye adsorption Process Plot (indicating the spontaneous reaction process).

Numerous studies have demonstrated that raising the temperature slows the biosorption process. This is known as an exothermic ($-\Delta H^\circ$) reaction because heat in the form of energy is released into the environment throughout the process (Cherif *et al.*, 2021). Alternatively, endothermic reactions absorb energy from the environment as heat (Hamdani *et al.*, 2020). The energy consumed during the bond formation between bacterial biomass and RR-120 dye during the endothermic process is less than bond-breaking energy (Abedi *et al.*, 2016). It is necessary to ascertain the biosorption process's spontaneity to compute the mechanism's Gibbs free energy (Abubakar and Sabo, 2020). In the presence of a specific temperature, a more considerable negative value ($-\Delta G^\circ$) indicates a favorable spontaneous biosorption process, whereas a positive Gibbs free energy change ($+\Delta G^\circ$) indicates a non-spontaneous, undesirable reaction process in the absence of a temperature. The type of reaction process, either physisorption or chemisorption, is also depicted in this manner (Srivastava *et al.*, 2015). The entropy change (ΔS°) in the reaction solution reflects how random the sorbate (dye) is in the reaction solution. In other words, the ΔS° value provides information regarding the rate at which a specific reaction proceeds compared to another individual reaction (Subbaiah and Kim, 2016).

Adsorption data errors considered within the context of the thermodynamic analytical framework include the dimensional discrepancy of fitted parameters, inappropriate calculation of

ΔH° and ΔS° , deceptive extrapolations about the spontaneity of a process, and the typical error of using ΔG and ΔG° interchangeably (Mudhoo and Pittman, 2023). When investigating adsorption thermodynamics, for computing purposes, the non-linear van't Hoff equation is now being proposed to find the correct ΔH° and ΔS° values. In order to compute the thermodynamic parameters that are characteristic of an adsorption process, the van't Hoff equation is often utilized (Mudhoo and Pittman, 2023).

Bacterial biomass characterization using Fourier transform infrared (FTIR) and scanning electron microscopy (SEM) techniques

A study on biosorbent structure and surface chemistry is required to develop dye adsorption processes. Dried microbial biomass contains roughly 50% carbon, almost all of which is present as one of the numerous reduced organic cell constituents. FTIR and SEM instruments were used to investigate the physicochemical characteristics of bacterial biomass biosorbent (Velkova *et al.*, 2018).

Fourier transform infrared (FTIR) analysis of Reactive Red 120 dye adsorption

The information provided by FTIR analysis helps identify unknown materials. It determines the infrared wavelength range the object being studied absorbs (Asfaram *et al.*, 2016). The Fourier transform, a mathematical technique that modifies a function by comparing amplitude

against frequency, can transform non-periodic functions. A spectrum plot was created for each study, with the x-axis representing wave numbers and the y-axis representing compound transmittances. The intensity of IR radiation is expressed as a percentage of the radiation that can pass through compared to a standard (Horciu *et al.*, 2020). For instance, a transmittance of one hundred percent indicates that the sample had absorbed the same amount of radiation as the reference. The radiation was completely absorbed when the sample had a transmittance value of 0%. The biosorption of dyes using bacterial biomass is founded on the characteristics of bacterial cell walls, which are made up of a wide variety of proteins, polysaccharides, and lipids, and offer a wide range of functional groups, including carboxylic, phosphate, hydroxyl, thiol and amino that can form interaction with dyes via various chemical reactions (Blaga *et al.*, 2021). FTIR analysis can be used to authenticate the biosorption process by observing the functional group and finding the bulk sites of adsorption (Nouri *et al.*, 2021).

The composition and functional group properties of unknown materials are usually analyzed using Fourier Transform Infrared (FTIR) spectroscopy. FTIR determines the wavelength range in the infrared region absorbed by the substance under consideration (Seo *et al.*, 2017). The Fourier transform, a mathematical approach that uses amplitude against frequency to change a function, can be used to transform non-periodic functions. For each study, a spectrum plot was created with the x-axis, with the y-axis representing the transmittances that are emitted by the compound and the x-axis representing the wavenumbers. When compared to a standard, the infrared (IR) radiation intensity is defined as the percentage of radiation that is able to pass through from the source (Alslaihi *et al.*, 2013). A one hundred percent transmittance indicates that the sample absorbed the same amount of radiation as the reference standard. The radiation was completely absorbed when the sample had a transmittance of 0%. Because of its high carbon content and lignocellulosic component, bacterial biomass has great potential as a material for the adsorption of dyes (Ong *et al.*, 2020). Active functional groups, such as those found in proteins, are responsible for determining the characteristics

of binding sites and the attachment of dyes directly to the surface of proteins, which include amino, sulfonate, carboxyl, hydroxyl, and carbonyl (Elsherif *et al.*, 2021). However, FTIR analysis helps to validate the biosorption process through the identification of adsorption binding sites (Wei *et al.*, 2016).

Low transmittance values indicate the occurrence of a more significant number of light-absorbing whereas high transmittance values indicate the presence of fewer bonds in the sample, with frequencies of vibration that are in accordance with the light that is coming in (Mona *et al.*, 2011). Proteins, nucleic acids, humic compound, polysaccharides and lipids are the richest chemical components in a bacterial biomass. They have assorted functional groups on their surfaces, connecting the sorbate ion and the molecules (Gupta and Devi, 2020). In order to determine whether or not the surface of the bacterial biomass contained many different functional groups, FTIR was utilized as a bulk detection method. Figure 13 below depicts several notable peaks for the RR-120 dye in the 4000-500 cm^{-1} wavenumber section. All of the peaks that were located in close proximity to the current peak were split into two distinct sections.: the first for the detection of the presence of an active group (1500 cm^{-1} to 4000 cm^{-1}) and another section is often used for the fingerprinting assessment of the molecule (peaks less than 1500 cm^{-1}). Figure 14 associates the spectrum of FTIR for *Enterobacter* sp. MM05 biomass at time before and after dye treatment with the corresponding 30 and 100 mg/L RR-120 dye.

Table 10 contains a peak position and probable FTIR Analysis of the Inter-atomic bond of isolated compounds. The FTIR analysis of raw bacterial biosorbent revealed numerous essential bands ranging from 4000 to 500 cm^{-1} . A strong and broad absorption band of hydroxyl occurred at 3191.23 cm^{-1} , implying the existence of -OH stretching, which depicts the presence of alcohols and phenols (hydrogen-bonded), N-H stretching of amines. The FTIR Peaks obtained at 2970.07 cm^{-1} imply C=O stretching of carboxylic acids, ketone, and C=C stretching of alkenes. The peak obtained at 2104.05 cm^{-1} implies the existence of C \equiv N/C \equiv C stretching of aldehyde/amines/nitriles (Bankole *et al.*, 2017).

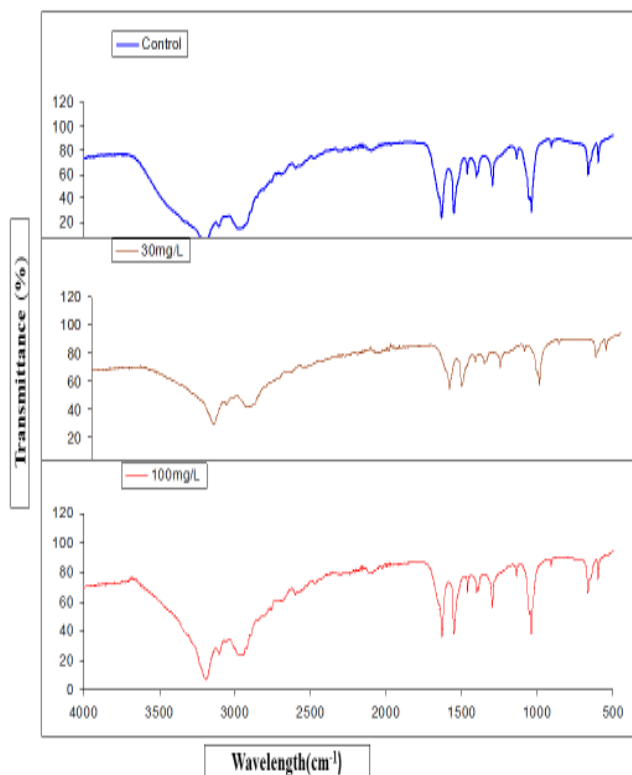


Figure 13. FTIR spectrum of the *Enterobacter* sp. MM05 Biomass before and after Treatment with 30 mg/L and 100 mg/L of RR-120 Dye.

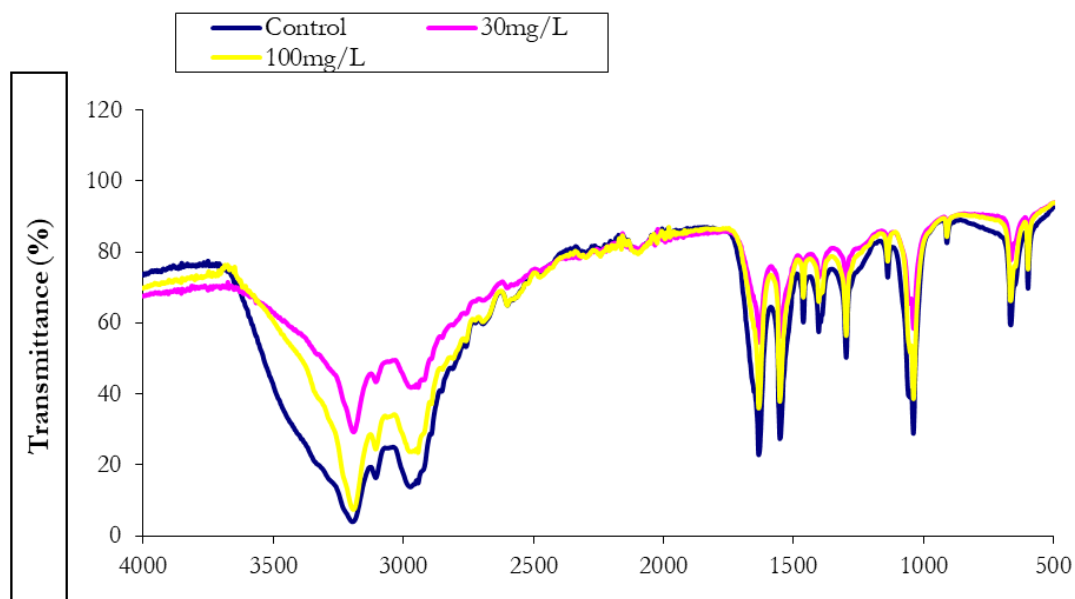


Figure 14. Comparison of FTIR spectrum of *Enterobacter* sp. MM05 biomass before and after treatment with 30 and 100 mg/L of RR-120 Dye

Table 10. Peak position and probable FTIR Analysis of Inter-atomic bond of Isolated Compounds from RR-120 Dye.

IR-absorption (cm ⁻¹)	Functional group
3191.23	O-H stretching vibration of alcohol and phenols
2970.7	C-H (Stretching), C=O stretching of carboxylic acid and ketone
2104.05	C≡N / C≡C stretching of aldehyde/amines/nitriles.
1632.98	C=C Stretching, N-H bending of primary amines, C=O Stretching of amide
1461.84	C-N stretching of aromatic amines C-H bonding
1296.95	C-O stretching of aryl ether and phenol and C-H stretching of aromatic hydrocarbons
1038.20	C-H stretching of aromatic hydrocarbon

The 1632.98 cm⁻¹ peak showed C=O stretching of aldehyde/ketone/ester/amides and C=O/C=C stretching of aromatic hydrocarbons, -NH stretching of amines and amides. The occurrence of hydrocarbon C-H/C=C bonding was denoted by the peak at 1448.5 cm⁻¹ (Aravind *et al.*, 2016). Observation of C-H bonding /C=C stretch and -the peak indicated C-H deformation /CH(CH₃) alkyl group at 1461.84 cm⁻¹ (Aravind *et al.*, 2016). Observation of C-O stretching of aryl ether and phenol and C-H stretching of aromatic hydrocarbon was indicated by the peak at 1296.95 cm⁻¹. Finally, the observation of aldehyde's C-O stretching was indicated by a peak at 1038.20 cm⁻¹ (Gurav *et al.*, 2021).

Scanning electron microscopy (SEM) analysis

Scanning electron microscopy is becoming increasingly valuable and essential as the size of materials decreases to accommodate more applications. In contrast to a light microscope, which employs visible light, SEM uses electrons for imaging. Scanning electron microscopy (SEM) scans the sample's specimen surfaces using a focused beam of electrons to generate images (Gurav *et al.*, 2021). In the process of electrons forming interactions with the atoms in the specimen, various signals are transmitted. These signals reveal information about the surface composition and structure of the specimen. These methods, along with several other methods like AFM or atomic force microscopy, can describe the process occurring during dye biosorption (Guo *et al.*, 2020). The samples were then dried,

washed, and grounded. This sample was then examined with an SEM/EDX analyzer at an appropriate resolution (× 5000 magnification) and micrographs were taken, as shown in Figure 15 (Zhuang *et al.*, 2011). An adsorption study conducted by (Nguyen *et al.*, 2016), employed SEM to inspect the bacterial surface morphology prior and post-adsorption shows that the biomass surface morphology is found to be heterogeneous, non-porous, and smooth. The images after treatment (Figure 15) exposed changes between the surface of the cells that comprise the bacterial biomass and the dye. The effect of dye absorption on the surface structure of bacterial mass is also variable depending on the dye concentration. At the initial stage or at moderate levels, small dyes, such as Reactive Red 120 (RR-120), do not interfere with the bacterium's surface. However, these dyes can also make an initially very irregular bacterial surface quite smooth at high levels. This has been seen in research where an enhanced dye concentration was seen to lead to the accumulation of dye particles covering an uneven surface and hence having a polished look. For example, (Mubarak *et al.*, 2017) found that RR-120 dye adsorption at high concentrations made chitosan beads have a smoother surface under SEM observation. Likewise, Islam and co-workers (Chakraborty *et al.*, 2021) observed that RR-120 dye adsorption on mahogany wood and bark charcoal made the adsorbents' surface smooth. These results indicate that the degree of alteration of surface morphology of bacterial for biomass dye adsorption depend on the dye's concentration.

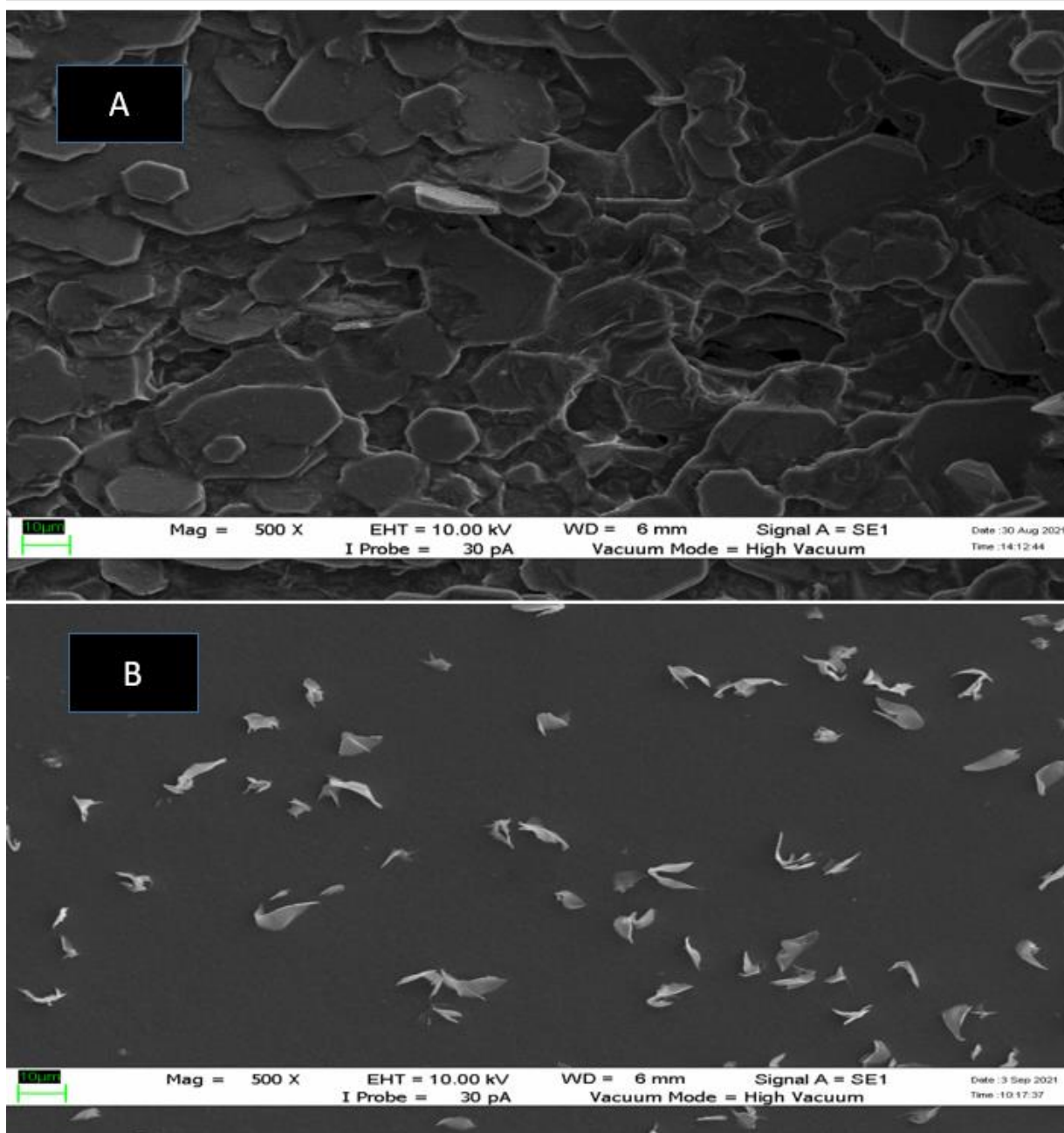


Figure 15. Scanning electron micrograph of *Enterobacter* sp. MMO5 biomass (A) Before Adsorption and (B) After Adsorption (Magnification: x5000).

CONCLUSION

The present research found that the *Enterobacter* sp. MMO5 biomass can remove Reactive Red 120 (RR-120) dye. The optimal conditions for adsorption were found to be at pH 4.0, 30 °C, 50 min contact time, and using 0.05 g of biomass. The adsorption process was optimized through the application of RSM with CCD, which

indicated a 9% increase in adsorption compared to OFAT. The Freundlich isotherm model was found to be a precise description of the data, whereas the PSO kinetic model was found to be the one that best defines the process of adsorption. According to the discoveries of thermodynamic studies, the process was found to be spontaneous, endothermic, and feasible at the temperatures that were experimented. According to the findings of the FTIR and SEM analyses, the

adsorption process was significantly affected by the functional groups and structure of the bacterial biomass. The findings of this study add to a better insight of the potential of microorganisms in bioremediation and exhibit the possibility of utilizing bacterial biomass to remove dyes.

ACKNOWLEDGEMENTS

The research is funded by the Ministry of Higher Education (MOHE) under the Fundamental Research Grant Scheme (FRGS/1/2019/STGO5/UPM/02/7).

CONFLICT OF INTEREST

The authors have declared that no conflict of interest exists.

REFERENCES

- Abedi S, Zavvar Mousavi H, Asghari A. 2016. Investigation of heavy metal ions adsorption by magnetically modified aloe vera leaves ash based on equilibrium, kinetic and thermodynamic studies. *Desalination and Water Treatment*. 57(29):13747–13759. <https://doi.org/10.1080/19443994.2015.1060536>.
- Abubakar A, Manogaran M, Yasid NA, et al. 2023. Equilibrium, kinetic and thermodynamic studies of the adsorption of trypan blue dye by *Pseudomonas* sp. strain MM02 inactivated biomass. *Korean J. Chem. Eng.* 40(8):1928–1953. <https://doi.org/10.1007/s11814-023-1450-y>.
- Abubakar A, Sabo IA. 2020. Thermodynamics Modelling of Lead (II) Biosorption using *Cystoseira stricta* BIO REMEDIATION SCIENCE AND TECHNOLOGY Thermodynamics Modelling of Lead (II) Biosorption using *Cystoseira stricta* Biomass. 8(December):21–23.
- Adamu FA, Basirun AA, Ismail AS, et al. 2023. BIOREMEDIATION SCIENCE AND TECHNOLOGY Isothermal Remodelling of the Biosorption of Congo Red onto Kaolin. 11(1):33–43.
- Ali F, Ali N, Bibi I, et al. 2020. Case Studies in Chemical and Environmental Engineering Adsorption isotherm, kinetics and thermodynamic of acid blue and basic blue dyes onto activated charcoal. 2(July):1–6. <https://doi.org/10.1016/j.cscee.2020.100040>.
- Alslaibi TM, Abustan I, Ahmad MA, et al. 2013. Cadmium removal from aqueous solution using microwaved olive stone activated carbon. *Journal of Environmental Chemical Engineering*. 1(3):589–599. <https://doi.org/10.1016/j.jece.2013.06.028>.
- Ameenudeen S, Unnikrishnan S, Ramalingam K. 2021. Statistical optimization for the efficacious degradation of reactive azo dyes using *Acinetobacter baumannii* JC359. *Journal of Environmental Management*. 279(October):111512. <https://doi.org/10.1016/j.jenvman.2020.111512>.
- Aragaw TA, Bogale FM. 2021. Biomass-Based Adsorbents for Removal of Dyes From Wastewater: A Review. *Frontiers in Environmental Science*. 9(December). <https://doi.org/10.3389/fenvs.2021.764958>.
- Aravind P, Selvaraj H, Ferro S, et al. 2016. An integrated (electro- and bio-oxidation) approach for remediation of industrial wastewater containing azo-dyes: Understanding the degradation mechanism and toxicity assessment. *Journal of Hazardous Materials*. 318:203–215. <https://doi.org/10.1016/j.jhazmat.2016.07.028>.
- Arica MY, Bayramoğlu G. 2007. Biosorption of Reactive Red-120 dye from aqueous solution by native and modified fungus biomass preparations of *Lentinus sajor-caju*. *Journal of Hazardous Materials*. 149(2):499–507. <https://doi.org/10.1016/j.jhazmat.2007.04.021>.
- Asfaram A, Ghaedi M, Ghezlbash GR, et al. 2016. Biosorption of malachite green by novel biosorbent *Yarrowia lipolytica* isf7: Application of response surface methodology. *Journal of Molecular Liquids*. 214:249–258. <https://doi.org/10.1016/j.molliq.2015.12.075>.
- Asgher M. 2012. Biosorption of reactive dyes: A review. *Water, Air, and Soil Pollution*. 223(5):2417–2435. <https://doi.org/10.1007/s11270-011-1034-z>.
- Baldikova E, Mullerova S, Prochazkova J, et al. 2019. Use of waste *Japonochytrium* sp. biomass after lipid extraction as an efficient adsorbent for triphenylmethane dye applied in aquaculture. *Biomass Conversion and Biorefinery*. 9(3):479–488. <https://doi.org/10.1007/s13399-018-0362-2>.
- Bankole PO, Adekunle AA, Obidi OF. 2017. Mycodecolorization of Reactive Red HE7B dye by *Achaetomium strumarium* and *Aspergillus flavus* and shelf life determination. *Cogent Environmental Science*. 3(1):1–14. <https://doi.org/10.1080/23311843.2017.1278646>.
- Basirun AA, Shukor MY. 2021. Kinetic Analysis of the Adsorption of Cibacron Blue onto Bean Peel. *Bulletin of Environmental Science and Sustainable Management* (e-ISSN 2716-5353). 5(2):14–18. <https://doi.org/10.54987/bessm.v5i2.649>.
- Bayramoglu G, Yilmaz M. 2018. Azo dye removal using free and immobilized fungal biomasses: Isotherms, Kinetics and thermodynamic studies. *Fibers and Polymers*. 19(4):877–886. <https://doi.org/10.1007/s12221-018-7875-y>.
- Bildik F, Turan GT, Barim G, et al. 2014. Removal of Acidic and Basic Dyes from Water using Crosslinked Polystyrene Based Quaternary Ethyl Piperazine Resin. *Separation Science and Technology (Philadelphia)*. 49(11):1700–1705. <https://doi.org/10.1080/01496395.2014.906462>.
- Bilehal DC, Kulkarni RM, Nandibewoor ST. 2001. Kinetics and mechanistic study of the ruthenium(III) catalyzed oxidative deamination and decarboxylation of L-valine by alkaline permanganate. *Canadian Journal of Chemistry*. 79(12):1926–1933. <https://doi.org/10.1139/cjc-79-12-1926>.
- Blaga AC, Zaharia C, Suteu D. 2021. Polysaccharides as support for microbial biomass-based adsorbents with applications in removal of heavy metals and dyes. *Polymers*. 13(17). <https://doi.org/10.3390/polym13172893>.
- Canizo B V., Agostini E, Wevar Oller AL, et al. 2019. Removal of Crystal Violet from Natural Water and Effluents Through Biosorption on Bacterial Biomass Isolated from Rhizospheric Soil. *Water, Air, and Soil Pollution*. 230(8). <https://doi.org/10.1007/s11270-019-4235-5>.
- Çelekli A, Bozkuş B, Bozkurt H. 2019. Development of a new adsorbent from pumpkin husk by KOH-modification to remove copper ions. *Environmental Science and Pollution Research*. 26(12):11514–11523. <https://doi.org/10.1007/s11356-017-1160-2>.

- Çelekli A, Çelekli F, Çiçek E, et al. 2014. Predictive modeling of sorption and desorption of a reactive azo dye by pumpkin husk. *Environmental Science and Pollution Research*. 21(7):5086–5097. <https://doi.org/10.1007/s11356-013-2452-9>.
- Çelekli A, Yavuzatmaca M, Bozkurt H. 2009. Kinetic and equilibrium studies on the adsorption of reactive red 120 from aqueous solution on *Spirogyra majuscula*. *Chemical Engineering Journal*. 152(1):139–145. <https://doi.org/10.1016/j.cej.2009.04.016>.
- Chakraborty T, Ghosh G, Akter M, et al. 2021. Biosorption of Reactive Red 120 Dye from Aqueous Solutions by using Mahagoni (Swietenia mahagoni) Wood and Bark *Charcoal: Equilibrium, and Kinetic Studies*. 7:905–921. <https://doi.org/10.22059/POLL.2021.325135.1110>.
- Chatterjee S, Lee MW, Wooa SH. 2010. Adsorption of congo red by chitosan hydrogel beads impregnated with carbon nanotubes. *Bioresource Technology*. 101(6):1800–1806. <https://doi.org/10.1016/j.biortech.2009.10.051>.
- Chen SH, Cheow YL, Ng SL, et al. 2020. Removal of triphenylmethane dyes in single-dye and dye-metal mixtures by live and dead cells of metal-tolerant *Penicillium simplicissimum*. *Separation Science and Technology (Philadelphia)*. 55(13):2410–2420. <https://doi.org/10.1080/01496395.2019.1626422>.
- Chen T, Da T, Ma Y. 2021. Reasonable calculation of the thermodynamic parameters from adsorption equilibrium constant. *Journal of Molecular Liquids*. 322:114980. <https://doi.org/10.1016/j.molliq.2020.114980>.
- Cheng Z, Feng K, Su Y, et al. 2020. Novel biosorbents synthesized from fungal and bacterial biomass and their applications in the adsorption of volatile organic compounds. *Bioresource Technology*. 300:122705. <https://doi.org/10.1016/j.biortech.2019.122705>.
- Cherif M, Rodrigues N, Veloso ACA, et al. 2021. Kinetic-thermodynamic study of the oxidative stability of Arbequina olive oils flavored with lemon verbena essential oil. *Lwt*. 140:110711. <https://doi.org/10.1016/j.lwt.2020.110711>.
- Cheruiyot GK, Wanyonyi WC, Kiplimo JJ, et al. 2019. Adsorption of toxic crystal violet dye using coffee husks: Equilibrium, kinetics and thermodynamics study. *Scientific African*. 5:1–11. <https://doi.org/10.1016/j.sciaf.2019.e00116>.
- Cope FW. 1972. Generalizations of the Roginsky-Zeldovich (or Elovich) equation for charge transport across biological surfaces. *The Bulletin of Mathematical Biophysics*. 34(3):419–427. <https://doi.org/10.1007/BF02476452>.
- Dan-Iya BI, Adamu FA, Ubana MA, et al. 2023. Mercury Sorption onto Rice Husk Ash: An Isothermal Remodelling. *Bioremediation Science and Technology Research* (2289-5892). 11(1):23–32. <https://doi.org/10.54987/bstr.v11i1.833>.
- Dan-Iya BI, Khayat ME, Shukor MY. 2023. Biosorption of Zn (II) onto Rice Husk Ash: Isothermal Remodelling. *Journal of Environmental Bioremediation and Toxicology*. 6(1):34–43. <https://doi.org/10.54987/jebat.v6i1.813>.
- Das A, Mishra S. 2017. Removal of textile dye reactive green-19 using bacterial consortium: Process optimization using response surface methodology and kinetics study. *Journal of Environmental Chemical Engineering*. 5(1):612–627. <https://doi.org/10.1016/j.jece.2016.10.005>.
- Değermenci GD, Değermenci N, Ayvaoglu V, et al. 2019. Adsorption of reactive dyes on lignocellulosic waste; characterization, equilibrium, kinetic and thermodynamic studies. *Journal of Cleaner Production*. 225:1220–1229. <https://doi.org/10.1016/j.jclepro.2019.03.260>.
- Dubinin MM. 1965. Modern state of the theory of volume filling of micropore adsorbents during adsorption of gases and steams on carbon adsorbents. *Zh. Fiz. Khim.* 39(6):1305–1317.
- Elsherif KM, El-dali A, Alkarewi AA, et al. 2021. Crystal violet absorption maxima. 7(2):79–89.
- Eris S, Azizian S. 2017. Analysis of adsorption kinetics at solid/solution interface using a hyperbolic tangent model. *Journal of Molecular Liquids*. 231:523–527. <https://doi.org/10.1016/j.molliq.2017.02.052>.
- Felista MM, Wanyonyi WC, Ongera G. 2020. Adsorption of anionic dye (Reactive black 5) using macadamia seed Husks: Kinetics and equilibrium studies. *Scientific African*. 7:e00283. <https://doi.org/10.1016/j.sciaf.2020.e00283>.
- Fomina M, Gadd GM. 2014. Biosorption: Current perspectives on concept, definition and application. *Bioresource Technology*. 160:3–14. <https://doi.org/10.1016/j.biortech.2013.12.102>.
- Fritz W, Schluender EU. 1974. Simultaneous adsorption equilibria of organic solutes in dilute aqueous solutions on activated carbon. *Chemical Engineering Science*. 29(5):1279–1282. [https://doi.org/10.1016/0009-2509\(74\)80128-4](https://doi.org/10.1016/0009-2509(74)80128-4).
- Gadd GM. 2009. Biosorption: Critical review of scientific rationale, environmental importance and significance for pollution treatment. *Journal of Chemical Technology and Biotechnology*. 84(1):13–28. <https://doi.org/10.1002/jctb.1999>.
- Giese EC, Silva DDV, Costa AFM, et al. 2020. Immobilized microbial nanoparticles for biosorption. *Critical Reviews in Biotechnology*. 40(5):653–666. <https://doi.org/10.1080/07388551.2020.1751583>.
- Gopalakrishnan Y, Al-Gheethi A, Malek MA, et al. 2020. Removal of basic brown 16 from aqueous solution using durian shell adsorbent, optimisation and techno-economic analysis. *Sustainability (Switzerland)*. 12(21):1–22. <https://doi.org/10.3390/su12218928>.
- Guo JJ, Huang XP, Xiang L, et al. 2020. Source, migration and toxicology of microplastics in soil. *Environment International*. 137(July 2019):105263. <https://doi.org/10.1016/j.envint.2019.105263>.
- Gupta KK, Devi D. 2020. Characteristics investigation on biofilm formation and biodegradation activities of *Pseudomonas aeruginosa* strain ISJ14 colonizing low density polyethylene (LDPE) surface. *Helvion*. 6(7):e04398. <https://doi.org/10.1016/j.helivon.2020.e04398>.
- Gurav R, Bhatia SK, Choi TR, et al. 2021. Application of macroalgal biomass derived biochar and bioelectrochemical system with *Shewanella* for the adsorptive removal and biodegradation of toxic azo dye. *Chemosphere*. 264:128539. <https://doi.org/10.1016/j.chemosphere.2020.128539>.
- Hamdani A, Amrane A, Kader Yettefi I, et al. 2020. Carbon and nitrogen removal from a synthetic dairy effluent in a vertical-flow fixed bed bioreactor. *Bioresource Technology Reports*. 12(September):100581. <https://doi.org/10.1016/j.biteb.2020.100581>.
- Ho YS. 2004. Citation review of Lagergren kinetic rate equation on adsorption reactions. *Scientometrics*. 59(1):171–177. <https://doi.org/10.1023/B:SCIE.0000013305.99473.cf>.
- Ho YS. 2006. Review of second-order models for adsorption systems. *Journal of Hazardous Materials*. 136(3):681–689. <https://doi.org/10.1016/j.jhazmat.2005.12.043>.
- Horciu IL, Blaga AC, Rusu L, et al. 2020. Biosorption of reactive dyes from aqueous media using the bacillus sp. Residual biomass. *Desalination and Water Treatment*. 195:353–360. <https://doi.org/10.5004/dwt.2020.25901>.
- Hu X, Chen C, Zhang D, et al. 2021. Kinetics, isotherm and chemical speciation analysis of Hg(II) adsorption over oxygen-containing MXene adsorbent. *Chemosphere*. 278:130206. <https://doi.org/10.1016/j.chemosphere.2021.130206>.
- Jafari AJ, Kakavandi B, Kalantary RR, et al. 2016. Application of mesoporous magnetic carbon composite for reactive dyes removal: Process optimization using response surface

- methodology. *Korean Journal of Chemical Engineering*. 33(10):2878–2890. <https://doi.org/10.1007/s11814-016-0155-x>.
- Karlapudi AP, Krupanidhi S, E. RR, et al. 2018. Plackett-Burman design for screening of process components and their effects on production of lactase by newly isolated *Bacillus* sp. VUVD101 strain from Dairy effluent. *Beni-Suef University Journal of Basic and Applied Sciences*. 7(4):543–546. <https://doi.org/10.1016/j.bjbas.2018.06.006>.
- Karthik V, Saravanan K, Sivarajasekar N, et al. 2016. Bioremediation of dye bearing effluents using microbial biomass. *Ecol. Environ. Conserv.* 22:S423–S434.
- Khammour F, Elkouali M, Kenz A, et al. 2016. A statistical approach based on the full factorial experiment for optimization of dyes adsorption on biomaterials prepared from mint and tea. *Journal of Materials and Environmental Science*. 7(4):1379–1385.
- Langmuir I. 1918. The adsorption of gases on plane surfaces of glass, mica and platinum. *Journal of the American Chemical Society*. 40(9):1361–1403. <https://doi.org/10.1021/ja02242a004>.
- Li Y, Du Q, Liu T, et al. 2013. Methylene blue adsorption on graphene oxide/calcium alginate composites. *Carbohydrate Polymers*. 95(1):501–507. <https://doi.org/10.1016/j.carbpol.2013.01.094>.
- Lim CK, Aris A, Neoh CH, et al. 2014. Evaluation of macrocomposite based sequencing batch biofilm reactor (MC-SBBR) for decolorization and biodegradation of azo dye Acid Orange 7. *International Biodeterioration and Biodegradation*. 87:9–17. <https://doi.org/10.1016/j.ibiod.2013.10.022>.
- Lim CK, Bay HH, Aris A, et al. 2013. Biosorption and biodegradation of Acid Orange 7 by *Enterococcus faecalis* strain ZL: Optimization by response surface methodological approach. *Environmental Science and Pollution Research*. 20(7):5056–5066. <https://doi.org/10.1007/s11356-013-1476-5>.
- Liu S, Lim M, Amal R. 2014. TiO₂-coated natural zeolite: Rapid humic acid adsorption and effective photocatalytic regeneration. *Chemical Engineering Science*. 105:46–52. <https://doi.org/10.1016/j.ces.2013.10.041>.
- Liu Y. 2008. New insights into pseudo-second-order kinetic equation for adsorption. *Colloids and Surfaces A: Physicochemical and Engineering Aspects*. 320(1–3):275–278. <https://doi.org/10.1016/j.colsurfa.2008.01.032>.
- Long J, Li H, Jiang D, et al. 2017. Biosorption of strontium(II) from aqueous solutions by *Bacillus cereus* isolated from strontium hyperaccumulator *Andropogon gayanus*. *Process Safety and Environmental Protection*. 111(Ii):23–30. <https://doi.org/10.1016/j.psep.2017.06.010>.
- Mahanty B, Behera SK, Sahoo NK. 2023. Misinterpretation of Dubinin–Radushkevich isotherm and its implications on adsorption parameter estimates. *Separation Science and Technology*. 58(7):1275–1282. <https://doi.org/10.1080/01496395.2023.2189050>.
- Mahendran S, Gokulan R, Aravindan A, et al. 2023. Production of *Ulva prolifera* derived biochar and evaluation of adsorptive removal of Reactive Red 120: batch, isotherm, kinetic, thermodynamic and regeneration studies. *Biomass Conversion and Biorefinery*. 13(6):5379–5390. <https://doi.org/10.1007/s13399-021-01483-0>.
- Mahmoud MS, Mostafa MK, Mohamed SA, et al. 2017. Bioremediation of red azo dye from aqueous solutions by *Aspergillus niger* strain isolated from textile wastewater. *Journal of Environmental Chemical Engineering*. 5(1):547–554. <https://doi.org/10.1016/j.jece.2016.12.030>.
- Manogaran M, Shukor MY, Yasid NA, et al. 2018. Optimisation of culture composition for glyphosate degradation by *Burkholderia vietnamiensis* strain AQ5-12. 3 *Biotech*. 8(2). <https://doi.org/10.1007/s13205-018-1123-4>.
- Manogaran M, Yasid NA, Othman AR, et al. 2021. Biodecolourisation of reactive red 120 as a sole carbon source by a bacterial consortium—toxicity assessment and statistical optimisation. *International Journal of Environmental Research and Public Health*. 18(5):1–26. <https://doi.org/10.3390/ijerph18052424>.
- Mawad AMM, Albasri H, Temerk HA. 2021. Biosorption of malachite green by dry cells of isolated free living nitrogen fixing bacteria. *Nature Environment and Pollution Technology*. 20(3):1217–1223. <https://doi.org/10.46488/NEPT.2021.V20I03.030>.
- Mohammadi N, Khani H, Gupta VK, et al. 2011. Adsorption process of methyl orange dye onto mesoporous carbon material-kinetic and thermodynamic studies. *Journal of Colloid and Interface Science*. 362(2):457–462. <https://doi.org/10.1016/j.jcis.2011.06.067>.
- Mona S, Kaushik A, Kaushik CP. 2011. Biosorption of reactive dye by waste biomass of *Nostoc linckia*. *Ecological Engineering*. 37(10):1589–1594. <https://doi.org/10.1016/j.ecoleng.2011.04.005>.
- Monte Blanco SPD, Scheufele FB, Módenes AN, et al. 2017. Kinetic, equilibrium and thermodynamic phenomenological modeling of reactive dye adsorption onto polymeric adsorbent. *Chemical Engineering Journal*. 307:466–475. <https://doi.org/10.1016/j.cej.2016.08.104>.
- Monte ML, Moreno ML, Senna J, et al. 2018. Moisture sorption isotherms of chitosan-glycerol films: Thermodynamic properties and microstructure. *Food Bioscience*. 22:170–177. <https://doi.org/10.1016/j.fbio.2018.02.004>.
- Moussout H, Ahlafi H, Aazza M, et al. 2018. Critical of linear and nonlinear equations of pseudo-first order and pseudo-second order kinetic models. *Karaba International Journal of Modern Science*. 4(2):244–254. <https://doi.org/10.1016/j.kijoms.2018.04.001>.
- Mu B, Xu L, Yang Y. 2023. Rational fabrication of completely amorphous chitosan-formyl-sucrose sorbents with excellent durability and regenerability for high-throughput dye removal. *Chemical Engineering Journal*. 461:1–36. <https://doi.org/10.1016/j.cej.2023.142134>.
- Mubarak NSA, Jawad AH, Nawawi WI. 2017. Equilibrium, kinetic and thermodynamic studies of Reactive Red 120 dye adsorption by chitosan beads from aqueous solution. *Energ. Ecol. Environ.* 2(1):85–93. <https://doi.org/10.1007/s40974-016-0027-6>.
- Mudhoo A, Pittman CU. 2023. Adsorption data modeling and analysis under scrutiny: A clarion call to redress recently found troubling flaws. *Chemical Engineering Research and Design*. 192:371–388. <https://doi.org/10.1016/j.cherd.2023.02.033>.
- Bin Mukhlsh MZ, Horie Y, Nomiya T. 2017. Flexible Alumina-Silica Nanofibrous Membrane and Its High Adaptability in Reactive Red-120 Dye Removal from Water. *Water, Air, and Soil Pollution*. 228(9). <https://doi.org/10.1007/s11270-017-3546-7>.
- Muthukumar C, Sivakumar VM, Thirumarimurugan M. 2016. Adsorption isotherms and kinetic studies of crystal violet dye removal from aqueous solution using surfactant modified magnetic nanoadsorbent. *Journal of the Taiwan Institute of Chemical Engineers*. 63:354–362. <https://doi.org/10.1016/j.jtice.2016.03.034>.
- Naskar A, Majumder R. 2017. Understanding the adsorption behaviour of acid yellow 99 on *Aspergillus niger* biomass. *Journal of Molecular Liquids*. 242:892–899. <https://doi.org/10.1016/j.molliq.2017.05.155>.
- Nath J, Das A, Ray L. 2015. Biosorption of Malachite Green from Aqueous Solution Using Resting and Immobilised Biomass

- of *Bacillus cereus* M116 (MTCC 5521). *Indian Chemical Engineer.* 57(1):82–100. <https://doi.org/10.1080/00194506.2014.997813>.
- Navai A, Yazdani M, Alidadi H, et al. 2019. Biosorption of reactive red 120 dye from aqueous solution using *Saccharomyces cerevisiae*: Rsm analysis, isotherms and kinetic studies. *Desalination and Water Treatment.* 171:418–427. <https://doi.org/10.5004/dwt.2019.24780>.
- Nguyen DT, Tran HN, Juang RS, et al. 2020. Adsorption process and mechanism of acetaminophen onto commercial activated carbon. *Journal of Environmental Chemical Engineering.* 8(6):104408. <https://doi.org/10.1016/j.jece.2020.104408>.
- Nguyen TA, Fu CC, Juang RS. 2016. Biosorption and biodegradation of a sulfur dye in high-strength dyeing wastewater by *Acidithiobacillus thiooxidans*. *Journal of Environmental Management.* 182:265–271. <https://doi.org/10.1016/j.jenvman.2016.07.083>.
- Nouri H, Azin E, Kamyabi A, et al. 2021. Biosorption performance and cell surface properties of a fungal-based sorbent in azo dye removal coupled with textile wastewater. *International Journal of Environmental Science and Technology.* 18(9):2545–2558. <https://doi.org/10.1007/s13762-020-03011-5>.
- Nwachukwu BC, Ayangbenro AS, Babalola OO. 2021. Elucidating the rhizosphere associated bacteria for environmental sustainability. *Agriculture (Switzerland).* 11(1):1–18. <https://doi.org/10.3390/agriculture11010075>.
- de Oliveira Carvalho C, Costa Rodrigues DL, Lima EC, et al. 2019. Kinetic, equilibrium, and thermodynamic studies on the adsorption of ciprofloxacin by activated carbon produced from Jerivá (*Syagrus romanzoffiana*). *Environmental Science and Pollution Research.* 26(5):4690–4702. <https://doi.org/10.1007/s11356-018-3954-2>.
- Ong HC, Chen WH, Singh Y, et al. 2020. A state-of-the-art review on thermochemical conversion of biomass for biofuel production: A TG-FTIR approach. *Energy Conversion and Management.* 209(December 2019):112634. <https://doi.org/10.1016/j.enconman.2020.112634>.
- Parker GR. 1995. Optimum isotherm equation and thermodynamic interpretation for aqueous 1,1,2-trichloroethene adsorption isotherms on three adsorbents. *Adsorption.* 1(2):113–132. <https://doi.org/10.1007/BF00705000>.
- Prola LDT, Acayanka E, Lima EC, et al. 2013. Comparison of *Jatropha curcas* shells in natural form and treated by non-thermal plasma as biosorbents for removal of Reactive Red 120 textile dye from aqueous solution. *Industrial Crops and Products.* 46:328–340. <https://doi.org/10.1016/j.indcrop.2013.02.018>.
- Radushkevich LV. 1949. Potential theory of sorption and structure of carbons. *Zhurnal Fizicheskoi Khimii.* 23:1410–1420.
- Redlich, Peterson. 1958. hydrochloric acid was then filtered through the fritted glass. Following this a 9.3. Notes. 63(1955):1958.
- Ribas MC, de Franco MAE, Adebayo MA, et al. 2020. Adsorption of Procion Red MX-5B dye from aqueous solution using homemade peach and commercial activated carbons. *Applied Water Science.* 10(6):1–13. <https://doi.org/10.1007/s13201-020-01237-9>.
- Ridha FN, Webley PA. 2009. Anomalous Henry's law behavior of nitrogen and carbon dioxide adsorption on alkali-exchanged chabazite zeolites. *Separation and Purification Technology.* 67(3):336–343. <https://doi.org/10.1016/j.seppur.2009.03.045>.
- Rizzi V, Longo A, Fini P, et al. 2014. Applicative Study (Part I): The Excellent Conditions to Remove in Batch Direct Textile Dyes (Direct Red, Direct Blue and Direct Yellow) from Aqueous Solutions by Adsorption Processes on Low-Cost Chitosan Films under Different Conditions. *Advances in Chemical Engineering and Science.* 04(04):454–469. <https://doi.org/10.4236/aces.2014.44048>.
- Rusu L, Grigoraş C-G, Simion A-I, et al. 2022. Biosorption Potential of Microbial and Residual Biomass of *Saccharomyces pastorianus* Immobilized in Calcium Alginate Matrix for Pharmaceuticals Removal from Aqueous Solutions. *Polymers.* 14(14):2855. <https://doi.org/10.3390/polym14142855>.
- Saha SP, Mazumdar D. 2019. Optimization of process parameter for alpha-amylase produced by *Bacillus cereus* amy3 using one factor at a time (OFAT) and central composite rotatable (CCRD) design based response surface methodology (RSM). *Biocatalysis and Agricultural Biotechnology.* 19:101168. <https://doi.org/10.1016/j.bcab.2019.101168>.
- Santhi T, Manonmani S, Vasantha VS, et al. 2016. A new alternative adsorbent for the removal of cationic dyes from aqueous solution. *Arabian Journal of Chemistry.* 9:S466–S474. <https://doi.org/10.1016/j.arabj.2011.06.004>.
- Santos SCR, Boaventura RAR. 2008. Adsorption modelling of textile dyes by sepiolite. *Applied Clay Science.* 42(1–2):137–145. <https://doi.org/10.1016/j.clay.2008.01.002>.
- Sarim KM, Kukreja K, Shah I, et al. 2019. Biosorption of direct textile dye Congo red by *Bacillus subtilis* HAU-KK01. *Bioremediation Journal.* 23(3):185–195. <https://doi.org/10.1080/10889868.2019.1641466>.
- Schirmer W. 1999. Physical Chemistry of Surfaces. *Zeitschrift für Physikalische Chemie.* 210(1):134–135. https://doi.org/10.1524/zpch.1999.210.part_1.134.
- Seo J, Hwang K, Lee S, et al. 2017. ST AC. Pharmaceutical Development and Technology. 0(0):000. <https://doi.org/10.1080/10837450.2017.1334664>.
- Sheshdeh RK, Nikou MRK, Badii K, et al. 2014. Equilibrium and kinetics studies for the adsorption of Basic Red 46 on nickel oxide nanoparticles-modified diatomite in aqueous solutions. *Journal of the Taiwan Institute of Chemical Engineers.* 45(4):1792–1802. <https://doi.org/10.1016/j.jtice.2014.02.020>.
- Shroff KA, Vaidya VK. 2011. Kinetics and equilibrium studies on biosorption of nickel from aqueous solution by dead fungal biomass of *Mucor hiemalis*. *Chemical Engineering Journal.* 171(3):1234–1245. <https://doi.org/10.1016/j.ccej.2011.05.034>.
- Silva CE de F, Gama BMV da, Gonçalves AH da S, et al. 2020. Basic-dye adsorption in albedo residue: Effect of pH, contact time, temperature, dye concentration, biomass dosage, rotation and ionic strength. *Journal of King Saud University - Engineering Sciences.* 32(6):351–359. <https://doi.org/10.1016/j.jksues.2019.04.006>.
- Singh KP, Gupta S, Singh AK, et al. 2011. Optimizing adsorption of crystal violet dye from water by magnetic nanocomposite using response surface modeling approach. *Journal of Hazardous Materials.* 186(2–3):1462–1473. <https://doi.org/10.1016/j.jhazmat.2010.12.032>.
- Solomon D, Kiflie Z, Van Hulle S. 2020. Using Box–Behnken experimental design to optimize the degradation of Basic Blue 41 dye by Fenton reaction. *International Journal of Industrial Chemistry.* 11(1):43–53. <https://doi.org/10.1007/s40090-020-00201-5>.
- Srinivasan A, Viraraghavan T. 2010. Decolorization of dye wastewaters by biosorbents: A review. *Journal of Environmental Management.* 91(10):1915–1929. <https://doi.org/10.1016/j.jenvman.2010.05.003>.
- Srivastava S, Agrawal SB, Mondal MK. 2015. Biosorption isotherms and kinetics on removal of Cr(VI) using native and chemically modified *Lagerstroemia speciosa* bark. *Ecological Engineering.* 85:56–66. <https://doi.org/10.1016/j.ecoleng.2015.10.011>.

- Subbaiah MV, Kim DS. 2016. Adsorption of methyl orange from aqueous solution by aminated pumpkin seed powder: Kinetics, isotherms, and thermodynamic studies. *Ecotoxicology and Environmental Safety*. 128:109–117. <https://doi.org/10.1016/j.ecoenv.2016.02.016>.
- Sulak MT, Yatmaz HC. 2012. Removal of textile dyes from aqueous solutions with eco-friendly biosorbent. *Desalination and Water Treatment*. 37(1–3):169–177. <https://doi.org/10.1080/19443994.2012.661269>.
- Taher T, Antini R, Saputri LI, et al. 2018. Removal of Congo red and Rhodamine B dyes from aqueous solution by raw Sarolangun bentonite: Kinetics, equilibrium and thermodynamic studies. *AIP Conference Proceedings*. 2049. <https://doi.org/10.1063/1.5082416>.
- Tan KL, Hameed BH. 2017. Insight into the adsorption kinetics models for the removal of contaminants from aqueous solutions. *Journal of the Taiwan Institute of Chemical Engineers*. 74:25–48. <https://doi.org/10.1016/j.jtice.2017.01.024>.
- Tran HN. 2022. Improper Estimation of Thermodynamic Parameters in Adsorption Studies with Distribution Coefficient $K_D(q_e/C_e)$ or Freundlich Constant (K F): Considerations from the Derivation of Dimensionless Thermodynamic Equilibrium Constant and Suggestions. *Adsorption Science and Technology*. 2022. <https://doi.org/10.1155/2022/5553212>.
- Tran HN, You SJ, Chao HP. 2016. Thermodynamic parameters of cadmium adsorption onto orange peel calculated from various methods: A comparison study. *Journal of Environmental Chemical Engineering*. 4(3):2671–2682. <https://doi.org/10.1016/j.jece.2016.05.009>.
- Tran HN, You SJ, Chao HP. 2017. Insight into adsorption mechanism of cationic dye onto agricultural residues-derived hydrochars: Negligible role of π - π interaction. *Korean Journal of Chemical Engineering*. 34(6):1708–1720. <https://doi.org/10.1007/s11814-017-0056-7>.
- Tran TH, Le AH, Pham TH, et al. 2020. Adsorption isotherms and kinetic modeling of methylene blue dye onto a carbonaceous hydrochar adsorbent derived from coffee husk waste. *Science of the Total Environment*. 725:138325. <https://doi.org/10.1016/j.scitotenv.2020.138325>.
- Vanaja K, Rani RHS. 2007. Design of experiments: Concept and applications of plackett burman design. *Clinical Research and Regulatory Affairs*. 24(1):1–23. <https://doi.org/10.1080/10601330701220520>.
- Velkova ZY, Kirova GK, Stoytcheva MS, et al. 2018. Biosorption of Congo Red and methylene blue by pretreated waste streptomyces fradiae biomass - Equilibrium, kinetic and thermodynamic studies. *Journal of the Serbian Chemical Society*. 83(1):107–120. <https://doi.org/10.2298/JSC170519093V>.
- Venkatraghavan R, Thiruchelvi R, Sharmila D. 2020. Statistical optimization of textile dye effluent adsorption by *Gracilaria edulis* using Plackett-Burman design and response surface methodology. *Helvion*. 6(10):e05219. <https://doi.org/10.1016/j.helivon.2020.e05219>.
- Vieth WR, Sladek KJ. 1965. A model for diffusion in a glassy polymer. *Journal of Colloid Science*. 20(9):1014–1033. [https://doi.org/10.1016/0095-8522\(65\)90071-1](https://doi.org/10.1016/0095-8522(65)90071-1).
- Vij RK, Janani VA, Subramanian D, et al. 2021. Equilibrium, kinetic and thermodynamic studies for the removal of Reactive Red dye 120 using *Hydrilla verticillata* biomass: A batch and column study. *Environmental Technology and Innovation*. 24:102009. <https://doi.org/10.1016/j.eti.2021.102009>.
- Wei D, Li M, Wang X, et al. 2016. Extracellular polymeric substances for Zn (II) binding during its sorption process onto aerobic granular sludge. *Journal of Hazardous Materials*. 301(September 2015):407–415. <https://doi.org/10.1016/j.jhazmat.2015.09.018>.
- Yahuza S, Sabo IA, Abubakar A, et al. 2020. Biosorption of Lead (II) Ions by Brown Algae: A Thermodynamic Study. 4(2):1–5.
- Zhang DH, Yang HM, Ou YJ, et al. 2017. Treatment of printing and dyeing wastewater by catalytic wet hydrogen peroxide oxidation of honeycomb cinder as carrier catalyst. *IOP Conference Series: Earth and Environmental Science*. 69(1). <https://doi.org/10.1088/1755-1315/69/1/012039>.
- Zhu HY, Jiang R, Xiao L. 2010. Adsorption of an anionic azo dye by chitosan/kaolin/ γ -Fe₂O₃ composites. *Applied Clay Science*. 48(3):522–526. <https://doi.org/10.1016/j.clay.2010.02.003>.
- Zhuang L, Zhou S, Yuan Y, et al. 2011. Development of *Enterobacter aerogenes* fuel cells: From in situ biohydrogen oxidation to direct electroactive biofilm. *Bioresour Technol*. 102(1):284–289. <https://doi.org/10.1016/j.biortech.2010.06.038>.